CRREL REPORT 91-16

Numerical Model for Forecasting Ice Conditions on the Ohio River

Hung Tao Shen, Goranka Bjedov, Steven F. Daly
and A.M. Wasantha Lal

September 1991

For conversion of SI metric units to U.S./British customary units of measurement consult ASTM Standard E380, Metric Practice Guide, *published by the American Society for Testing and Materials, 1916 Race St., Philadelphia, Pa. 19103.*

Cover: Ice in the pool at Emsworth Lock and Dam on the Ohio River.

CRREL Report 91-16

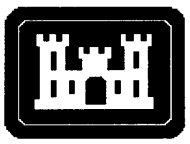

U.S. Army Corps of Engineers
Cold Regions Research & Engineering Laboratory

Numerical Model for Forecasting Ice Conditions on the Ohio River

Hung Tao Shen, Goranka Bjedov, Steven F. Daly
and A.M. Wasantha Lal

September 1991

Prepared for
OFFICE OF THE CHIEF OF ENGINEERS

PREFACE

This report was prepared by Hung Tao Shen, Professor of Civil and Environmental Engineering, Clarkson University; Goranka Bjedov, Graduate Assistant, Clarkson University; Steven F. Daly, Research Hydraulic Engineer, U.S. Army Cold Regions Research and Engineering Laboratory (CRREL); and A.M. Wasantha Lal, Graduate Assistant, Clarkson University. The report was technically reviewed by Dr. George D. Ashton of CRREL and Deborah H. Lee of the Detroit District of the U.S. Army Corps of Engineers. This study was conducted under the support of the CRREL–Clarkson Joint Graduate Research Program in Ice Engineering. Funding for this research was provided by the Office of the Chief of Engineers under the River Ice Management program, Work Unit CW32227, *Forecasting Ice Conditions on Inland Rivers*. The support and encouragement of Guenther E. Frankenstein is deeply appreciated. The authors acknowledge the assistance of George McKee of the Ohio River Division of the U.S. Army Corps of Engineers in providing information for hydraulic computations.

CONTENTS

ILLUSTRATIONS

TABLES

Numerical Model for Forecasting Ice Conditions on the Ohio River

HUNG TAO SHEN, GORANKA BJEDOV, STEVEN F. DALY AND A. M. WASANTHA LAL

INTRODUCTION

During the winter in areas of higher latitude, ice can form in rivers. The presence of ice can significantly influence flow and navigation conditions in the river. The ability to forecast river ice conditions is therefore of great importance in planning winter flow regulation and navigation operations.

The ice condition in a river not only influences, but also interacts with, its flow condition. Numerous computer models simulate unsteady flow in rivers under open-water conditions (Mahmood and Yevjevich 1975, Cunge et al. 1980, Fread 1985). Yapa and Shen (1986) developed an unsteady flow model for ice-covered rivers by including the effects of hydraulic resistance of the ice cover. In the model the transport of moving ice in the river and the ice cover formation were not considered, although the thermal growth and decay of the ice cover were simulated using a degree-day model. A few models are capable of simulating river ice conditions (Marcotte 1981, Michel and Drouin 1981, Petryk 1981, Calkins 1984, Shen and Yapa 1984). Except for that of Shen and Yapa (1984), all of these models use a backwater computation and ignore the distribution and transport of ice along the river. For long rivers subject to repeated freezing and melting during a winter, a river ice model must simulate the transport process correctly. In this study a numerical model called RICEOH for simulating river ice and flow conditions is developed for the Ohio River system between Pittsburgh, Pennsylvania, and Meldahl, Ohio. With weather forecasts as input, the model can be used to forecast river ice conditions.

The model is based on a single-channel river ice model recently developed by Lal (1988). In the hydraulics computation the one-dimensional unsteady flow model developed by Chen and Simons (1975) and implemented for the Ohio River under open-water conditions (Johnson 1982) is used. Modifications are made in the unsteady flow model to include the hydraulic resistance of the ice cover. In the ice model the water temperature and ice concentration distributions along the river are calculated by a Lagrangian–Eulerian scheme. The formation of the ice cover is modeled using existing equilibrium ice jam theories (Pariset and Hausser 1961). The thermal growth and decay of the ice cover are computed based on quasi-steady thermal conduction in the ice cover considering heat exchanges between the atmosphere, the ice cover and the underlying river water (Shen and Lal 1986). Modifications are made on the single-channel model of Lal (1988) to make the model applicable to a river system with dendritic tributaries.

HYDRAULIC ANALYSIS

The continuity and momentum equations for a river with a floating ice cover, as shown in Figure 1, are given as

$$\frac{\partial Q}{\partial x} + \frac{\partial A}{\partial t} - q_l = 0 \tag{1}$$

$$\rho \frac{\partial Q}{\partial t} + \rho \left(\frac{2Q}{A} \frac{\partial Q}{\partial x} - \frac{Q^2}{A^2} \frac{\partial A}{\partial x} \right) + \rho g A \frac{\partial H}{\partial x} + (p_i \tau_i + p_b \tau_b) - p q_l v_l = 0 \tag{2}$$

where Q = discharge
A = flow area
x = horizontal distance along the channel
t = time
q_l = lateral inflow to the channel
H = water level ($H = z_b + d_w + h_{su}$)
y = depth of the water ($y = d_w + h_{su}$)
g = acceleration due to gravity
z_b = bed elevation
ρ = density of water
d_w = depth of the flow
p_b = wetted perimeter formed by the channel bed
p_i = wetted perimeter formed by the ice cover
τ_b = shear stress at the channel bottom
τ_i = shear stress at the ice/water interface
v_l = lateral inflow velocity component in the main stream direction
h_{su} = submerged thickness of the ice cover.

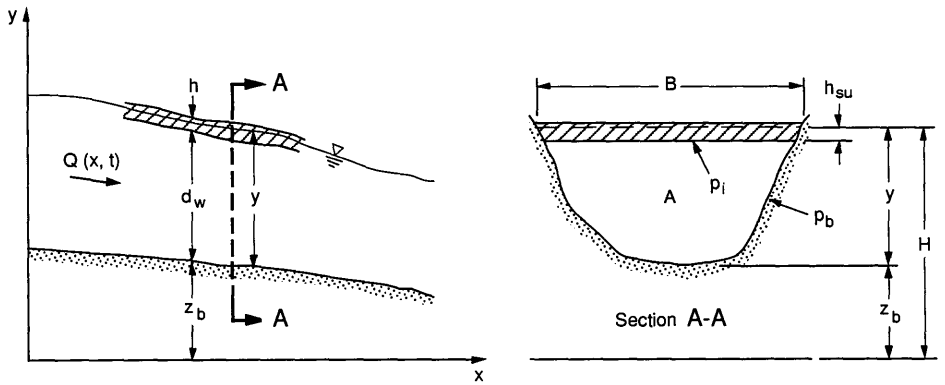

Figure 1. Channel flow with a floating ice cover.

Since eq 1 and 2 do not in general possess analytical solutions, one must rely on numerical techniques to solve them. In the present study the computer model developed for the Ohio River by Chen and Simons (1975) and Johnson (1982) is adopted to solve eq 1 and 2, with modifications for the terms related to the effect of the ice cover. The numerical method used is a linear implicit finite-difference method with a double-sweep algorithm.

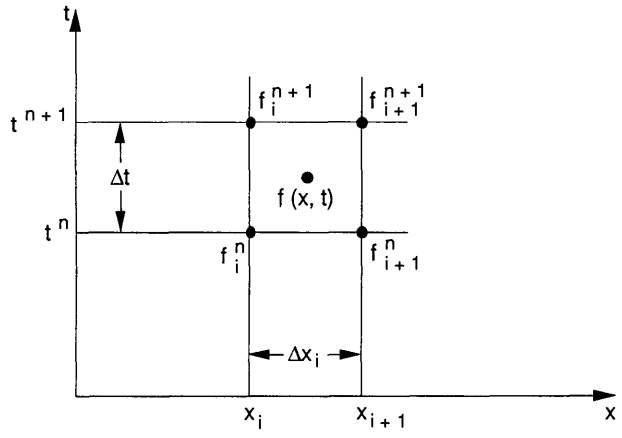

Figure 2. Four-point implicit scheme.

Finite-difference formulation

Figure 2 and eq 3 show the discretization of dependent variables and its derivatives in time and space:

$$f(x,t) = \frac{1}{4}\left(f_{i+1}^{n+1} + f_i^{n+1} + f_{i+1}^{n} + f_i^{n}\right)$$

$$\frac{\partial f}{\partial x} = \frac{\left(f_{i+1}^{n+1} - f_i^{n+1} + f_{i+1}^{n} - f_i^{n}\right)}{2\Delta x} \tag{3}$$

$$\frac{\partial f}{\partial t} = \frac{\left(f_{i+1}^{n+1} - f_{i+1}^{n} + f_i^{n+1} - f_i^{n}\right)}{2\Delta t}$$

where Δt is the time step used in computations and Δx is the distance between two neighboring points.

We can rearrange the one-dimensional flow equations in the following form:

$$B\frac{\partial d_w}{\partial t} + \frac{\partial Q}{\partial x} - q_l = 0 \tag{4}$$

and

$$\frac{\partial Q}{\partial t} + 2u\frac{\partial Q}{\partial x} - u^2 B\frac{\partial d_w}{\partial x} + gA\frac{\partial y}{\partial x} = gA\left(S_o - S_f\right) + q_l v_l + u^2\left(\frac{\partial A}{\partial x}\right)_{d_w = constant} \tag{5}$$

where B is the channel width, $u = Q/A$ is the averaged cross-sectional velocity and S_o and S_f represent the channel-bed slope and energy slope, respectively. According to eq 3 these equations can be written in finite-difference form as

$$\frac{1}{2\Delta x}\left[\left(Q_{i+1}^{n} - Q_i^{n}\right) + \left(Q_{i+1}^{n+1} - Q_i^{n+1}\right)\right] + B_{i+\frac{1}{2}}^{n}\frac{1}{2\Delta t}\left\{\left[\left(d_w\right)_i^{n+1} - \left(d_w\right)_i^{n}\right]\right.$$

$$\left. + \left[\left(d_w\right)_{i+1}^{n+1} - \left(d_w\right)_{i+1}^{n}\right]\right\} - \left(q_l\right)_{i+\frac{1}{2}}^{n+\frac{1}{2}} = 0 \tag{6}$$

and

$$\frac{1}{2\Delta t}\left[Q_i^{n+1} - Q_i^{n} + Q_{i+1}^{n+1} - Q_{i+1}^{n}\right] + u_{i+\frac{1}{2}}^{n}\frac{1}{\Delta x}\left[-Q_i^{n+1} - Q_i^{n} + Q_{i+1}^{n+1} + Q_{i+1}^{n}\right]$$

$$-\left(u^2 B\right)_{i+\frac{1}{2}}^{n} \frac{1}{2\Delta x}\left[\left(d_w\right)_{i+1}^{n} - \left(d_w\right)_{i}^{n} + \left(d_w\right)_{i+1}^{n+1} - \left(d_w\right)_{i}^{n+1}\right]$$

$$+ gA_{i+\frac{1}{2}}^{n} \frac{1}{2\Delta x}\left[y_{i+1}^{n} - y_{i}^{n} + y_{i+1}^{n+1} - y_{i}^{n+1}\right]$$

$$= g\left[AS_o\right]_{i+\frac{1}{2}}^{n} - gA_{i+\frac{1}{2}}^{n}\left(S_f\right)_{i+\frac{1}{2}}^{n+\frac{1}{2}} + \left(q_l u\right)_{i+\frac{1}{2}}^{n} + \left(u^2 A_x^{d_w}\right)_{i+\frac{1}{2}}^{n}. \tag{7}$$

In eq 6 and 7, $f_{i+\frac{1}{2}} = \frac{1}{2}\left(f_i^n + f_{i+1}^n\right)$ and $A_x^{d_w} = \left(\partial A/\partial x\right)_{d_w = constant}$. If the spatial grid has different lengths, then Δx in the above equations has to be replaced by Δx_i.

The presence of an ice cover can affect the frictional slope. For a reach as shown in Figure 3, the friction slope is expressed as

$$S_{f,i} = \alpha'_{o,i}\left(S_f\right)_{o,i} + \alpha'_{i,i}\left(S_f\right)_{i,i} \tag{8}$$

where $\alpha'_{o,i}$ and $\alpha'_{i,i}$ are the length fractions of open water and ice cover, respectively, in the length element Δl_i corresponding to node i.

The friction slope of the open-water portion can be calculated as

$$\left(S_f\right)_{o,i} = \frac{\left(n_{o,i} Q_{o,i}\right)^2}{\left(1.486 A_{o,i} R_{o,i}^{2/3}\right)^2} \tag{9}$$

where the hydraulic radius is defined as

$$R_{o,i} = \frac{A_{o,i}}{P_{o,i}}. \tag{10}$$

The subscript o represents the open-water conditions with no ice cover effects, and

$P_{o,i}$ = wetted perimeter of node i
$A_{o,i}$ = flow area at node i
$n_{o,i}$ = Manning's roughness coefficient of the channel bed for node i
u_o = velocity at node i.

The friction slope of an ice-covered reach is defined as

$$\left(S_f\right)_{i,i} = \frac{\left(n_{c,i} Q_{i,i}\right)^2}{\left(1.486 A_{i,i} R_{i,i}^{2/3}\right)^2} \tag{11}$$

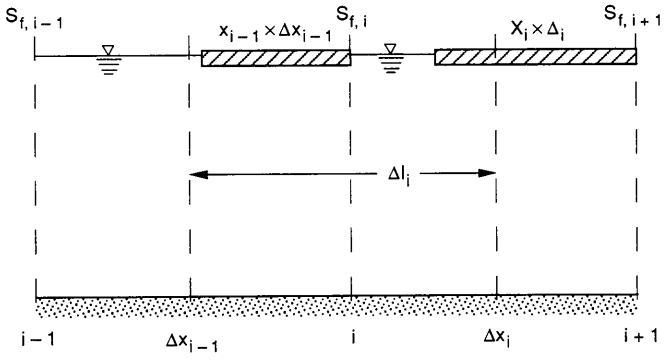

Figure 3. Definition sketch for the friction slope calculation.

where the composite roughness coefficient for node i is

$$n_{c,i} = \left[\frac{1}{2}\left(N_{i,i}^{3/2} + N_{o,i}^{3/2}\right)\right]^{2/3} \tag{12}$$

where $n_{i,i}$ is the undersurface roughness of the ice cover for node i.

The length fraction $\alpha'_{i,i}$ is calculated as

$$\alpha'_{i,i} = 2\,\frac{\alpha_i \Delta x_i + \alpha_{i-1}\,\Delta x_{i-1}}{\Delta x_i + \Delta x_{i-1}} \tag{13}$$

where coefficients α are defined in Figure 3:

$$\begin{aligned} \alpha_{i-1} &= X(i-1) && \text{for} && X(i-1) < 0.5 \\ &= 0.5 && \text{for} && X(i-1) > 0.5 \\ \alpha_i &= 0 && \text{for} && X(i) < 0.5 \\ &= X(i)-0.5 && \text{for} && X(i) > 0.5 \end{aligned}$$

and X_i and X_{i-1} = fractions of the length covered by ice in reaches i and $i-1$, namely the length of the ice cover divided by the length of the corresponding reach

$h_{su,i}$ and $h_{su,i-1}$ = submerged thicknesses of ice cover in reaches i and $i-1$, respectively

Δx_i and Δx_{i-1} = lengths of reaches i and $i-1$, respectively

i, $i-1$ and $i+1$ = nodal point indices.

The length fraction $\Delta x_{o,i}$ is

$$\Delta x_{o,i} = 1 - \Delta x_{i,i}. \tag{14}$$

The velocity for the fully ice-covered condition is expressed as

$$u_{i,i} = \frac{Q_i}{A_{i,i}} \tag{15}$$

where the flow area $A_{i,i}$ is given as

$$A_{i,i} = A_i - T_i\, h_{su,i}. \tag{16}$$

The equivalent submerged ice thickness for node i is defined as

$$h'_{su,i} = \frac{\alpha_{i-1}\,\Delta x_{i-1}\,h_{su,i-1} + \alpha_i\,\Delta x_i\,h_{su,i}}{\alpha_{i-1}\Delta x_{i-1} + \alpha_i \Delta x_i} \tag{17}$$

and the hydraulic radius for the ice-covered case is

$$R_{i,i} = \frac{A_{i,i}}{P_{i,i}} \tag{18}$$

where the wetted perimeter in the ice-covered case $P_{i,i} = P_{o,i} + T_i - 2h_{su,i}$, with T_i being the top width of the channel at node i. The equivalent ice cover roughness coefficient at node i is calculated from

$$n_{i,i} = \frac{\alpha_{i-1}\,\Delta x_{i-1}\,r_{i-1} + \alpha_i\,\Delta x_i\,r_i}{\alpha_{i-1}\Delta x_{i-1} + \alpha_i \Delta x_i} \tag{19}$$

where r_i and r_{i-1} are ice cover roughness coefficients for reaches i and i–1, respectively.

For the boundary node of each tributary, eq 17–19 are modified accordingly. For the upstream boundary node $\alpha'_{i,i} = 2(X_1 - 0.5)$ for $X_1 > 0.5$ and 0 otherwise, and the equivalent submerged thickness and roughness of ice cover are $h'_{su,I} = h_{su,I-1}$ and $n_{i,1} = r_1$. For the downstream boundary node these parameters are defined as $\alpha'_{i,I} = 2X_{I-1}$ for $X_{I-1} < 0.5$ and 1 otherwise, and $h'_{su,I} = h_{su,I-1}$ and $n_{i,I} = r_{I-1}$, where the subscript I denotes the last downstream node on the branch.

To assure the stability of the numerical scheme (Strelkoff 1970), the friction slope S_f is taken on t^{n+1} time level with a first-order Taylor expansion. A suitable expression for S_f^{n+1} is

$$[S_f(Q, y, X)]_i^{n+1} = (S_f)_i^n + \left(\frac{\partial S_f}{\partial Q}\right)_i^n \left(Q_i^{n+1} - Q_i^n\right)$$

$$+ \left(\frac{\partial S_f}{\partial y}\right)_i^n \left(y_i^{n+1} - y_i^n\right) + \left(\frac{\partial S_f}{\partial \alpha'_i}\right)_i^n \left(\alpha'^{n+1}_{i,i} - \alpha'^{n}_{i,i}\right) \tag{20}$$

where $\alpha'_{i,i}$ is defined in eq 13. Since the length fraction of an ice cover $\alpha'^{n+1}_{i,i}$ is unknown at the present time step, it is necessary to approximate the last term in eq 20. The approximation that was used in this model is

$$\alpha'^{n+1}_{i,i} - \alpha'^{n}_{i,i} = \alpha'^{n}_{i,i} - \alpha'^{n-1}_{i,i} .$$

Using eq 8–19, terms in eq 20 can be expressed as eq 21–23 considering n as a function of Q and y:

$$\frac{\partial S_f}{\partial Q} = 2(S_f)_o \left(\frac{1}{Q} + \frac{1}{n_o}\frac{\partial n_o}{\partial Q}\right)\alpha'_o + 2(S_f)_i \left(\frac{1}{Q} + \frac{1}{n_c}\frac{\partial n_c}{\partial Q}\right)\alpha'_i \tag{21}$$

$$\frac{\partial S_f}{\partial y} = -2(S_f)_o \left[\frac{1}{A_o}\left(\frac{5}{3}T_o - \frac{2}{3}R_o\frac{dP_o}{dy}\right) - \frac{1}{n_o}\frac{\partial n_o}{\partial y}\right]\alpha'_o$$

$$-2(S_f)_i \left[\frac{1}{A_i}\left(\frac{5}{3}T_i - \frac{2}{3}R_i\frac{dP_i}{dy}\right) - \frac{1}{n_c}\frac{\partial n_c}{\partial y}\right]\alpha'_i \tag{22}$$

and

$$\frac{\partial S_f}{\partial \alpha'_i} = (S_f)_i - (S_f)_o . \tag{23}$$

Substituting eq 10–13 into eq 6 and 7 yields

$$-\theta Q_i + (C_1)_i y_i + \theta Q_{i+1} + (C_1)_i y_{i+1} = (C_2)_i \tag{24}$$

and

$$(C_3)_i Q_i + (C_4)_i Q_{i+1} + (C_5)_i y_i + (C_6)_i y_{i+1} = (C_7)_i \tag{25}$$

where $\theta = \dfrac{\Delta t}{\Delta x}$

$$(C_1)_i = \frac{1}{2}\left(T_i^n + T_{i+1}^n\right)$$

$$(C_2)_i = -\theta\left(Q_{i+1}^n - Q_i^n\right) + \left(C_1\right)_i\left(y_i^n + Y_{i+1}^n\right) + \Delta t\left[(q_l)_{i+\frac{1}{2}}^n + (q_l)_{i+\frac{1}{2}}^{n+1}\right]$$

$$(C_3)_i = 1 - 2CS1 + g\Delta t\left(\frac{S_f}{u}\right)_i^n + g\Delta t\left(CK3\right)$$

$$(C_4)_i = 1 + 2CS1 + g\Delta t\left(\frac{S_f}{u}\right)_{i+1}^n + g\Delta t\left(CK4\right)$$

$$(C_5)_i = CS2 - CS3 - g\Delta t\left(CK1\right)$$

$$(C_6)_i = -CS2 + CS3 - g\Delta t\left(CK2\right)$$

$$\begin{aligned}(C_7)_i = {} & Q_i^n + Q_{i+1}^n - 2\left(CS1\right)\left[Q_{i+1}^n - Q_i^n\right] + \left(CS2 - CS3\right)\left(y_{i+1}^n - y_i^n\right) \\ & + g\theta\left(A_i^n + A_{i+1}^n\right)\left(Z_i^n - Z_{i+1}^n\right) - \Delta t\left\{g\left[\left(CK1\right)y_i^n + \left(CK2\right)y_{i+1}^n - \left(CK3\right)Q_i^n\right.\right. \\ & \left.\left. - \left(CK4\right)Q_{i+1}^n\right] - \left[\left(u^2\right)_i^n + \left(u^2\right)_{i+1}^n\right]\left(A_x^y\right)_{i+\frac{1}{2}}^n - \frac{1}{2}\left[(q_1 u)_{i+\frac{1}{2}}^n + (q_1 u)_{i+\frac{1}{2}}^{n+1}\right]\right\} \\ & - \left[\left(S_f\right)_i - \left(S_f\right)_o\right]_i^n\left(\Delta x_{i,i}^n - \Delta x_{i,i}^{n-1}\right) - \left[\left(S_f\right)_i - \left(S_f\right)_o\right]_{i+1}^n\left(\Delta x_{i,i+1}^n - \Delta x_{i+1,i}^n\right)\end{aligned}$$

$$CS_1 = \frac{\theta}{2}\left(u_i^n + u_{i+1}^n\right)$$

$$CS_2 = \frac{\theta}{2}\left[\left(u^2T\right)_i^n + \left(u^2T\right)_{i+1}^n\right]$$

$$CS_3 = g\,\frac{\theta}{2}\left[\left(A_i^n + A_{i+1}^n\right)\right]$$

$$\begin{aligned}CK_1 = {} & \left[\left(S_f\right)_o\left(\frac{5T_o}{3} - \frac{2R_o}{3}\,\frac{dP_o}{dy} - \frac{A_o}{n_o}\frac{\partial n_o}{\partial y}\right)\right]_i^n \Delta x_{o,i}^n \\ & + \left[\left(S_f\right)_i\left(\frac{5T_i}{3} - \frac{2R_i}{3}\,\frac{dP_i}{dy} - \frac{A_i}{n_c}\frac{\partial n_c}{\partial y}\right)\right]_i^n \Delta x_{i,i}^n\end{aligned}$$

$$\begin{aligned}CK_2 = {} & \left[\left(S_f\right)_o\left(\frac{5T_o}{3} - \frac{2R_o}{3}\,\frac{dP_o}{dy} - \frac{A_o}{n_o}\frac{\partial n_o}{\partial y_o}\right)\right]_{i+1}^n \Delta x_{o,i+1}^n \\ & + \left[\left(S_f\right)_i\left(\frac{5T_i}{3} - \frac{2R_i}{3}\,\frac{dP_i}{dy} - \frac{A_i}{n_c}\frac{\partial n_c}{\partial y}\right)\right]_{i+1}^n \Delta x_{i,i+1}^n\end{aligned}$$

$$CK_3 = \left[(S_f)_o \left(\frac{A_o}{n_o}\frac{\partial n_o}{\partial Q}\right)\right]_i^n \Delta x_{o,i}^n + \left[(S_f)_o \left(\frac{A_i}{n_c}\frac{\partial n_c}{\partial Q}\right)\right]_i^n \Delta x_{i,i}^n$$

$$CK_4 = \left[(S_f)_i \left(\frac{A_o}{n_o}\frac{\partial n_o}{\partial Q}\right)\right]_{i+1}^n \Delta x_{o,i+1}^n + \left[(S_f)_i \left(\frac{A_i}{n_c}\frac{\partial n_c}{\partial Q}\right)\right]_{i+1}^n \Delta x_{i,i+1}^n .$$

All coefficients in eq 24 and 25 are evaluated at the time level t^n and therefore are known.

There are four unknowns in eq 24 and 25 at the time level t^{n+1}. However, two unknowns are common for any two neighboring grid points. Consequently the (I–1) pairs of equations contain $2I$ unknowns. Therefore, we need two additional equations that can be established from boundary conditions to complete this system.

At the upstream boundary it is assumed that the flood hydrograph supplies the flow depth or discharge as a function of time. This relation can be written as

$$C_9 Q_1 + C_{10} y_1 = C_{11} . \tag{26}$$

At the downstream boundary the rating curve is expressed in segmentized form as

$$C_{12} Q_I + C_{13} y_I = C_{14} . \tag{27}$$

Equations 24–27 form a system of $2I$ linear algebraic equations with $2I$ unknowns. Any standard method can be used for its solution. In this model the double-sweep algorithm was used.

Double-sweep algorithm

If we rearrange eq 24 and 25 by subtracting from them the same set of equations from the previous time step, we get

$$H_y \Delta y_{i+1} + B_i \Delta Q_{i+1} = C_i \Delta y_i + D_i \Delta Q_i + G_i \tag{28}$$

$$H_y' \Delta y_{i+1} + B_i' \Delta Q_{i+1} = C_i' \Delta y_i + D_i' \Delta Q_i + G_i' \tag{29}$$

where $\Delta y_i = y_i^{n+1} - y_i^n$ and $\Delta Q_i = Q_i^{n+1} - Q_i^n$.

Assume now that there is a linear relationship of the type

$$\Delta Q_i = E_i \Delta y_i + F_i \tag{30}$$

for point i. It can be easily proven that an analogous linear relationship exists for the next point i+1 and a recurrence relationship, eq 31, can be obtained (Liggett and Cunge 1975):

$$\Delta Q_{i+1} = E_{i+1} \Delta y_{i+1} + F_{i+1} . \tag{31}$$

Coefficients E_{i+1} and F_{i+1} can be computed if E_i and F_i are known. If we now substitute eq 30 in eq 28, we can get

$$\Delta y_i = L_i \Delta y_{i+1} + M_i \Delta Q_{i+1} + N_i \tag{32}$$

where $L_i = \dfrac{H_i}{C_i + D_i E_i}$

$$M_i = \frac{B_i}{C_i + D_i E_i}$$

$$N_i = \frac{G_i + D_i F_i}{C_i + D_i E_i}.$$

Equation 31 permits the computation of Δy_i when the increments Δy_{i+1} and ΔQ_{i+1} are known. Therefore, it is possible to compute y^{n+1} and Q^{n+1} for all points of a given reach. This method is fully explained in the block diagram of Figure 4. The interaction between the main river and a tributary and the treatment of locks and dams are explained in detail by Johnson (1982). The practical meaning of the double-sweep algorithm is that the number of elementary operations needed to solve the system is proportional to the number of points I. Standard methods, such as matrix inversion, have the number of operations proportional to I^3 (Burden and Faires 1986).

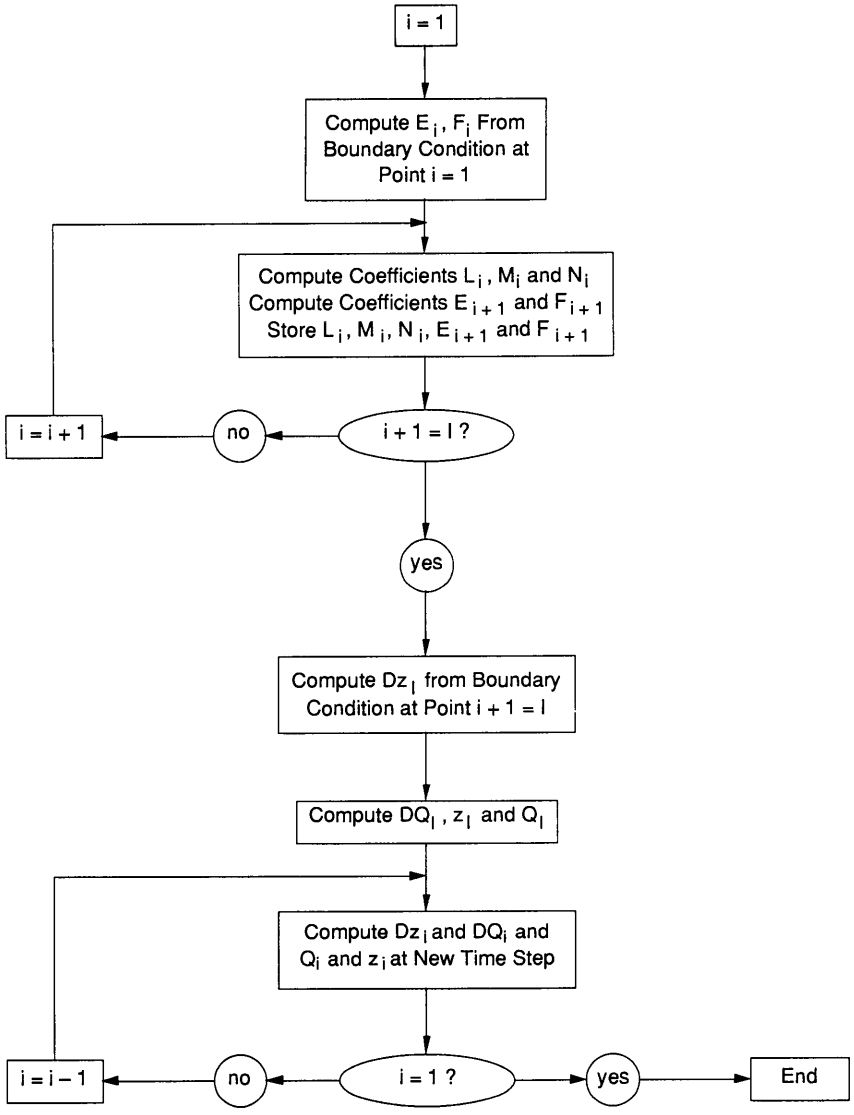

Figure 4. Block diagram for the double-sweep algorithm.

After the flow conditions at the time level t^{n+1} are computed for each node by solving eq 4 and 5, the temperature and ice conditions are calculated along the river. The procedures for thermal and ice computations are described in the following section.

SIMULATION OF THERMAL AND ICE CONDITIONS

The present model adopts the model developed by Lal (1988) to simulate thermal and ice conditions, with some modifications.

Water temperature and ice discharge distributions

In a well-mixed river the governing equation for the distribution of water temperature T_w along the river is

$$\frac{\partial}{\partial t}\left(\rho C_p A T_w\right) + \frac{\partial}{\partial x}\left(Q \rho C_p T_w\right) = \frac{\partial}{\partial x}\left(A E_x \rho C_p \frac{\partial T_w}{\partial x}\right) + B\Phi + q_l \rho C_p \left(T_l - T_w\right) \quad (33)$$

where A = flow area
B = river width
ρ = density of water
C_p = specific heat of water
E_x = longitudinal dispersion coefficient
Φ = heat flux per unit surface area of the river
T_l = temperature of the lateral inflow.

On the river surface the energy flux consists of solar or short-wave radiation, long-wave radiation, heat transfer due to evaporation or condensation, sensible heat transfer due to conduction, and heat transfer due to precipitation. A simplified linear model is used in this study. The net heat exchange at the free surface is expressed as (Ashton 1986)

$$\Phi = h_{wa}\left(T_a - T_w\right) \quad (34)$$

where T_w = water temperature
T_a = air temperature
h_{wa} = heat exchange coefficient at the water/air interface.

Linear models cannot accurately describe the heat exchange process. However, for rivers where extensive weather data are not available, they provide sufficiently accurate prediction of water temperature.

When a river is covered with ice, the turbulent heat exchange between the river water and the ice cover is described by (Ashton 1986)

$$\Phi_{wi} = h_{wi}\left(T_w - T_m\right) \quad (35)$$

where T_m is the melting temperature (0°C) and h_{wi} is the turbulent heat exchange coefficient given as

$$h_{wi} = C_{wi}\frac{u^{0.8}}{d_w^{0.2}} \quad (36)$$

where the coefficient C_{wi} approximately equals 1622 W $s^{0.8}$ $m^{-2.6}$ $°C^{-1}$. Laboratory and field investigations indicate that C_{wi} may increase with the resistance of the ice cover.

When the water temperature drops to the freezing point T_f, frazil ice production starts in a river. The equation for frazil ice transport can be written as

$$\frac{\partial}{\partial t}\left(\rho_i L_i C_i\right) + \frac{\partial}{\partial x}\left(Q\,\rho_i L_i C_i\right) = \frac{\partial}{\partial x}\left(AE_x\,\rho_i L_i \frac{\partial C_i}{\partial x}\right) + B h_{wa}\left(T_a - T_f\right) \tag{37}$$

where C_i = ice concentration
L_i = latent heat of fusion
ρ_i = density of ice.

Since eq 37 is in the same form as eq 33, the solution of eq 33 when $T_w < 0°C$ can be used to determine the ice concentration by setting $T_w = T_f$ in eq 34 and letting $C_i = \rho C_p T_w / \rho_i L_i$ in the solution.

If we neglect the dispersion term, eq 33 can be reduced to eq 38 by using the continuity equation (eq 1):

$$A\frac{\partial}{\partial t}\left(\rho C_p T_w\right) + Q\frac{\partial}{\partial x}\left(\rho C_p T_w\right) = B\Phi + q_l\,\rho\,C_p\left(T_l - T_w\right). \tag{38}$$

In Lagrangian form eq 38 becomes

$$\frac{DT_w}{Dt} = \frac{\Phi}{\rho C_p d_w} + \frac{q_l\left(T_l - T_w\right)}{A}. \tag{39}$$

In the present model eq 39 is solved using a Lagrangian–Eulerian scheme. In this scheme parcels of water with known water temperature or ice concentration at time t^n are followed along the river to obtain the temperature or ice concentration distribution at $t^n+\Delta t$. As shown in Figure 5, a water parcel located at x_i at t^n will move to a new location at time $t^n+\Delta t$. The x coordinate of this new location is given by

$$s_i = x_i + \sum_{k=1}^{j-1} \Delta x_{i-1+k} + u_j\left(\Delta t - \sum_{k=1}^{j-1} \delta t_k\right) \tag{40}$$

where s_i = new position of the particle
$\delta t_k = \Delta x_k / u_k$ = travel time of the parcel in k^{th} reach
$j-1$ = last node passed by the moving parcel.

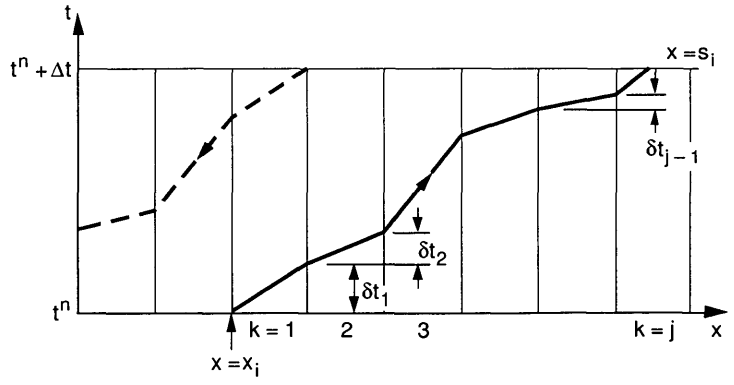

Figure 5. The Lagrangian–Eulerian scheme.

The water temperature of the parcel can be obtained by numerically integrating eq 39:

$$(T_w)_i^{(n+1)} = (T_w)_i^n - \sum_{k=1}^{j-1} \left(\frac{\Phi}{\rho C_p d_{wk}} + \frac{q_l \left[T_l - (T_w)_k^n \right]}{A} \right) \delta t_k$$

$$- \left(\frac{\Phi}{\rho C_p d_{wj}} + \frac{q_l \left[T_l - (T_w)_j^n \right]}{A} \right) \left(\Delta t - \sum_{k=1}^{j-1} \delta t_k \right) \tag{41}$$

where $(T_w)_i^{(n+1)}$ is the temperature of the water parcel, which was originally located at x_i, and d_{wk} is the mean depth of reach k. At the end of each time step, the water temperature at every grid point is obtained by linearly interpolating from the closest Lagrangian parcels upstream and downstream of the grid point. These interpolated values will be used as starting points for the next time step. An outline of the procedure is given in Figure 5.

When Δt is large, the water parcel originated from the upstream boundary at time t^n can travel over several grid points. There will be no Lagrangian parcels located in the upstream portion of the river for interpolation. Water temperatures of nodal points in this region are determined by tracing back in time to the upstream boundary, where the original temperatures of water parcels are known at all times.

When calculating the water temperature for the first node in the main stream downstream of a junction, instantaneous mixing of water from the tributary with that of the main stream is assumed:

$$T_{w3} = \frac{T_{w1} Q_{w1} + T_{w2} Q_{w2}}{Q_{w1} + Q_{w2}} \tag{42}$$

where Q_{w1} and Q_{w2} = discharges in the main stream and the tributary, respectively
T_{w1} and T_{w2} = water temperatures in the main stream and the tributary immediately upstream of the junction
T_{w3} = water temperature in the main stream immediately downstream of the junction.

Ice cover formation

The initial ice cover formation is a process governed by channel geometry, hydraulic conditions, surface ice supply and ice properties. Depending on these conditions, different modes of ice cover formation can occur on the river. The present model is capable of simulating ice cover formation by particle juxtaposition, hydraulic thickening (narrow jam formation) and mechanical thickening (wide jam formation). After the ice cover is initiated, it will progress upstream, depending on the thickness of the ice cover and the supply of ice suspended in water. When the ice cover progresses to a junction, it can progress into both the tributary and the main stream. During this process the ice cover can change its thickness due to thermal growth or decay and deposition or erosion of frazil ice underneath the ice cover.

In regions with low flow velocity, ice covers can form by simple juxtaposition of ice floes. The stability condition for incoming ice floes at the leading edge is given by (Ashton 1974)

$$\frac{v_c}{\left[g t_i \left(1 - \frac{\rho_i}{\rho} \right) \right]^{\frac{1}{2}}} = \frac{2\left(1 - \frac{t_i}{y} \right)}{\left[5 - 3\left(1 - \frac{t_i}{y} \right)^2 \right]^{\frac{1}{2}}} \tag{43}$$

where v_c = critical velocity upstream of the leading edge for underturning and submergence
t_i = thickness of the ice floe
y = upstream flow depth at the leading edge.

Another expression has been obtained earlier by Pariset and Hausser (1961):

$$F_{rc} = \frac{v_c}{\sqrt{gy}} = F\left(\frac{t_i}{l_i}\right)\left(1 - \frac{t_i}{y}\right)\sqrt{2\left(\frac{\rho - \rho_i}{\rho}\right)(1 - e)\frac{t_i}{y}} \tag{44}$$

where $F(t_i/l_i)$ = form factor, which varies between 0.6 and 1.3
l_i = length of the ice floe
e = porosity of the ice floe.

More recently, Daly and Axelson (1990) presented a refined formulation for the juxtaposition phenomenon. If the criterion for juxtaposition is satisfied, the ice cover will progress upstream with the same thickness as the incoming ice floes.

Field observations (Kivisild 1959) indicated that F_{rc} can vary from 0.05 to 0.10, depending on the floe characteristics. Since analytical formulas for F_{rc} require the geometry of the ice floe, it is difficult to apply them to field problems. In the present model the value of the critical Froude number F_{rc} is considered to be an input parameter that specifies the limiting condition for the juxtaposition mode. Floe thickness t_i and porosity e, which are needed in determining the rate of progression, are also specified.

When the Froude number becomes greater than the critical Froude number, the ice cover will progress as a narrow jam or by hydraulic thickening. Incoming floes will submerge and become deposited on the underside of the ice cover to a thickness governed by the flow condition.

To obtain the thickness of an ice cover in the hydraulic thickening mode, it is necessary to consider the interaction between the ice cover formation and the flow condition. If we apply the energy equation between sections 1 and 3 on Figure 6, we get

$$y_1 + \frac{u_1^2}{2g} = d_{w3} + \frac{u_3^2}{2g} + \frac{p_3}{\rho g}. \tag{45}$$

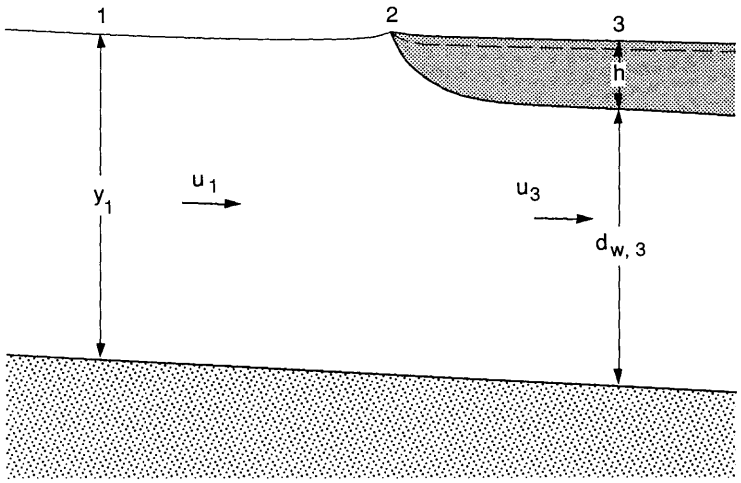

Figure 6. Definition sketch for the narrow jam formulation.

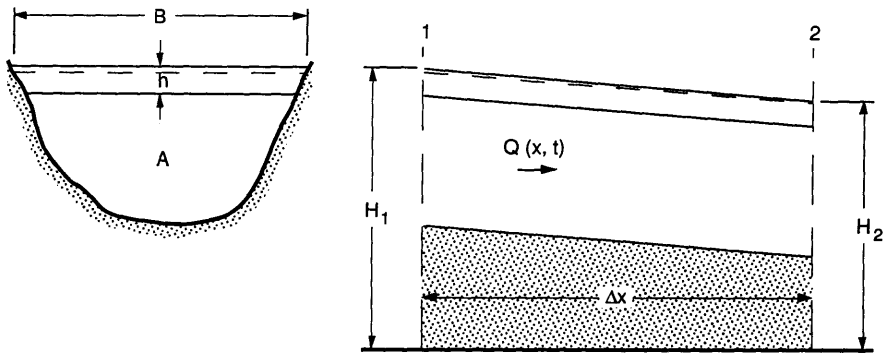

Figure 7. Definition sketch for an ice-covered reach.

A no-spill condition at section 2 gives

$$y_1 + \frac{u_1^2}{2g} < d_{w3} + h. \tag{46}$$

Using a hydrostatic condition the pressure underneath the ice cover at section 3, p_3, can be obtained from

$$p_3 = \rho g h - (1 - e)(\rho - \rho_i) g h. \tag{47}$$

By substituting eq 45 and 46 into eq 47 we obtain the first equation for A and h:

$$F_1(A, h) = Q^2 - 2gA^2\left(1 - \frac{\rho_i}{\rho}\right)h = 0. \tag{48}$$

Since the water level interacts with the thickening of the ice cover, an additional equation is needed for A and h. An equation for hydraulic conditions is obtained by applying the energy equation between points 1 and 2 of Figure 7:

$$H_1 + \frac{Q^2}{2gA_1^2} = H_2 + \frac{Q^2}{2gA_2^2} + S_f \Delta x. \tag{49}$$

If we express the net flow area as

$$A = A' - B\frac{\rho_i}{\rho} h \tag{50}$$

where A' is the known flow area corresponding to the depth of the flow y, and substitute for S_f in the eq 49, we can obtain a hydraulics backwater equation:

$$F_2(A, h) = 0. \tag{51}$$

Equations 48 and 51 are solved simultaneously for A and h using a Newton–Raphson procedure. In the narrow jam mode, there is a limiting Froude number $F_{r,max}$ beyond which ice cover cannot progress. The value of $F_{r,max}$, which typically equals 0.09, is considered to be an input to this model.

If the net streamwise force exceeds the internal resistance of the ice cover formed by hydraulic thickening, the cover will collapse and thicken until an equilibrium thickness is reached. This process is commonly known as mechanical thickening of an ice cover, or "shoving," and accumulations formed in this manner are often called wide river jams. When shoving occurs on the river, a relatively

long reach of ice cover will collapse, and the leading edge will move downstream. Based on the analyses of Pariset and Hausser (1961) and Uzuner and Kennedy (1976), an equation for the equilibrium thickness of wide jam t for a steady uniform flow can be obtained as follows:

$$\left[f_i + \frac{\rho_i}{\rho}\left(f_b + f_i\right)\frac{h}{d_w}\right]\frac{U^2 B}{8g} = \frac{2\tau_c h}{\rho g} + \mu\left(1 - e_p\right)\left(1 - \frac{\rho_i}{\rho}\right)\frac{\rho_i h^2}{\rho} \tag{52}$$

where f_i and f_b are Darcy–Weisbach friction factors related to the ice cover and the channel bed. Bank resistance per unit length of the ice cover is expressed as $\tau_c h + \mu F_s$, where $\tau_c h$ is the contribution due to cohesion and μF_s is the ice-over-ice friction term, with F_s being the streamwise force per unit width of the cover. Equation 52 was derived by assuming that the flow conditions when the ice cover reaches equilibrium thickness are known. Since this is not the case, a solution technique taking into consideration the interaction between the flow conditions and the ice cover formation was developed (Lal 1988).

Consider the case of an equilibrium ice jam condition in which the variables do not change along the river. Balancing the external forces acting on the ice cover by the bank resistance yields

$$2\left(\tau_c h + \mu_1 f\right)\Delta x = \left(\tau_i + \tau_g\right) B \Delta x \tag{53}$$

where f = longitudinal stress of the ice cover
τ_i = bottom friction due to the flow
τ_g = component of the weight in the direction of the slope of the cover
μ_1 = friction coefficient of ice to the banks
τ_c = cohesive strength of the bank.

Assuming that the maximum longitudinal force will occur at a passive state, it can be expressed as

$$f = \rho_i\left(1 - \frac{\rho_i}{\rho}\right)\frac{g h^2}{2} K_2 \tag{54}$$

where $K_2 = \left(1 - e\right)\tan^2\left(\frac{\pi}{4} + \frac{\Phi}{2}\right)$
Φ = internal friction angle of the ice accumulation
e = porosity of the ice cover.

The friction on the undersurface of the ice cover can be expressed as

$$\tau_i = \rho g \left(\frac{n_i}{n_c}\right)^{1.5} R S_f \tag{55}$$

and the weight component in the direction of the slope of the cover can be expressed as

$$\tau_g = \rho_i g h S_f . \tag{56}$$

Using eq 53–55 and substituting in the equilibrium condition of eq 52, we obtain the following:

$$F_3\left(A, h\right) = \mu\frac{\rho_i}{\rho}\left(1 - \frac{\rho_i}{\rho}\right)h^2 B^2 + \frac{2\tau_c B^2 h}{\gamma}$$

$$- 2^{1/3}\frac{Q^2 n_c^2 B^{10/3}}{A^{7/3}}\left[\left(\frac{n_i}{n_c}\right)^{3/2} + 2\frac{\rho_i}{\rho}\frac{hB}{A}\right] = 0 \tag{57}$$

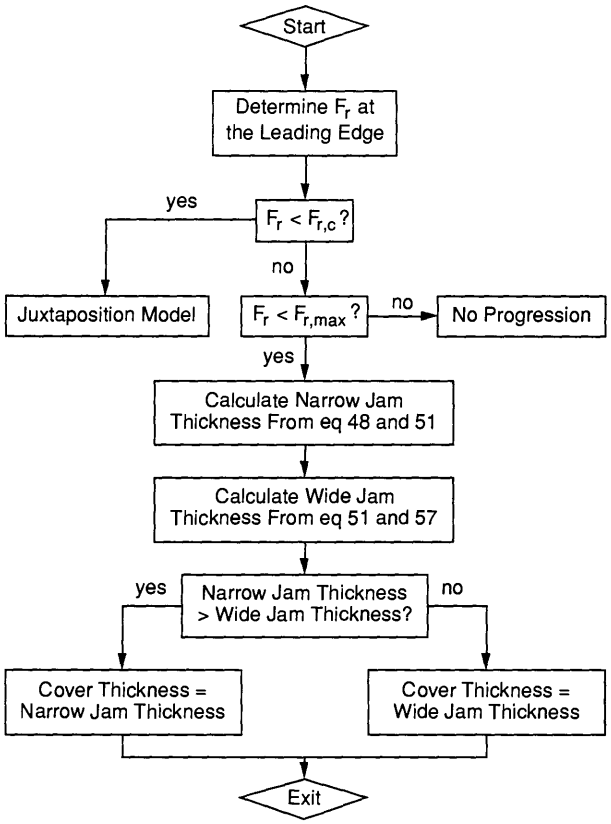

Figure 8. Block diagram for determining the initial ice cover thickness.

This equation has to be solved simultaneously with the backwater equation (eq 51) using the Newton–Raphson procedure to obtain A and h. The starting values of A and h for the iterative process can be obtained either from the previous time step or by the approximate solution obtained from eq 52. As a result of interaction, progression is possible over a wider range of conditions than allowed by eq 52. A simple flow chart outlining the calculation of the initial ice cover thickness is presented in Figure 8.

The ice cover can progress as a result of the obstruction of the ice flow due to natural or artificial causes. At an existing leading edge or obstruction, the surface fraction α_c of the incoming ice discharge will collect on its upstream side to lengthen the cover. The computational procedure to determine the increase in ice cover length x_p can be illustrated by Figure 9. Figure 9a describes the condition at time t^n. The concentration profile $C(x,t^n)$ is represented by A_1A. Figure 9b describes the ice condition at t^{n+1}. During the time interval Δt, the water parcel A, originally located at the leading edge X_L^n, will move to A'. The curve A'_1A represents the concentration profile at t^{n+1}, ignoring production and surface accumulation. This profile is a result of advection of the profile A_1A. Due to production in the open water area, the concentration profile $C'(x,t^{n+1})$ at t^{n+1}, ignoring surface accumulation only, is represented by $A'B'C'A_2$. The dotted area represents the ice produced during Δt. Since an α_c fraction of the ice that is passing through the leading edge will contribute to the ice cover progression, a shaded area $A'C'D'E'$ is used to represent the ice consumption for cover progression. In the Lagrangian scheme the profile $C'(x,t^{n+1})$ is first obtained by ignoring the consumption of surface ice. The ice in the shaded area $A'C'D'E'$ is then retrieved to form the ice cover between X_L^n and X_L^{n+1}. The final concentration profile $C(x,t^{n+1})$ at t^{n+1} is represented by $A_2C'D'E'A'$.

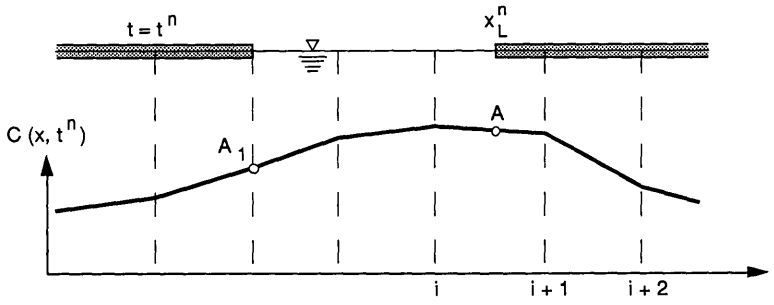

a. Condition at time t^n.

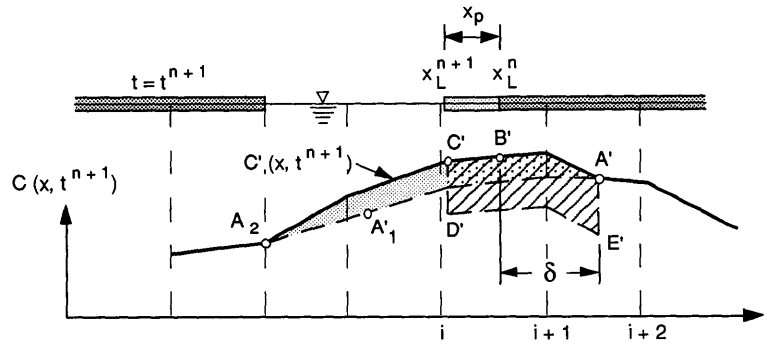

b. Condition at time t^{n+1}.

Figure 9. Definition sketch for ice cover progression.

Letting V_c represent the surface fraction of the ice passing through X_L, the length of the progression x_p can be obtained by equating the volume of the ice supply for the cover progression $V_c + \alpha_c x_p C_p A_p$ and the volume of the ice in the cover $Bhx_p(1-e_c)$:

$$x_p = \frac{V_c}{Bh(1-e_c) - \alpha_c C_p A_p} \tag{58}$$

where h = thickness of the newly formed ice cover
e_c = porosity of the ice cover
C_p = ice concentration
A_p = average flow area
α_c = fraction of ice discharge going into ice cover formation.

Ice particles that remain in suspension will travel under the ice cover after they pass the leading edge. Because of the insulation of the ice cover, further frazil production stops. The remaining ice continues to rise towards the underside of the cover under the influence of buoyancy and turbulent diffusion. As a result, ice particles will be deposited along the underside of the ice cover when possible. Frazil deposition changes the ice cover thickness and influences hydraulics. During the deposition process, the flow velocity is increasing due to the reduction in flow area. The deposition will cease when the velocity reaches a critical velocity of deposition. Deposited frazil ice erodes when the local flow velocity increases beyond a critical velocity of erosion. Erosion and deposition can take place in different parts of a river at the same time.

The rate at which the frazil ice is supplied to the underside accumulation of the ice cover, due to the upward movement of ice in the suspension, can be formulated by considering the mass balance of suspended frazil ice mass:

$$\frac{\partial(AC)}{\partial t} + \frac{\partial(QC)}{\partial x} = -\alpha^d v_b^d C^d B \tag{59}$$

where α^d is the probability of deposition of an ice particle that reaches the ice/water interface and $v_b^d C^d$ is the buoyant velocity and concentration at the ice/water interface. Assuming $\alpha^d v_b^d C^d = \alpha v_b C$ and applying the continuity equation, eq 59 can be written as

$$A\frac{\partial C}{\partial t} + Q\frac{\partial C}{\partial x} = -\alpha v_b C B. \tag{60}$$

In Lagrangian form this equation becomes

$$\frac{DC}{Dt} = -\alpha \frac{v_b C B}{A}. \tag{61}$$

Hence, the decrease in ice concentration ΔC in the suspension over a travel distance Δx is

$$\Delta C = C_1\left[1 - \exp\left(-\frac{\alpha v_b B \Delta x}{Au}\right)\right]. \tag{62}$$

Equation 62 calculates the supply of frazil ice to the underside of the cover. Deposition under any section of the ice cover is limited by a critical flow velocity v_{dep}^c. When the thickness of the frazil accumulation changes, the hydraulic condition will change correspondingly. The current version of the model assumes that the water level of the river does not change due to deposition and erosion, but the ice cover will float freely.

Based on this assumption the limiting condition for deposition thickness becomes

$$h_f \leq h_{fo} + \frac{\rho_f}{\rho_w}\left(\frac{A_o}{B} - \frac{Q}{Bv_{dep}}\right) \tag{63}$$

where A = flow area
h_f = thickness of frazil accumulation
ρ_f = density of frazil accumulation
o = subscript representing the condition at the beginning of the time step.

Erosion of frazil ice takes place when the local flow velocity over a frazil deposition increases beyond a certain value v_{ero}. The limiting thickness of frazil ice after erosion can be determined by using an expression similar to eq 63:

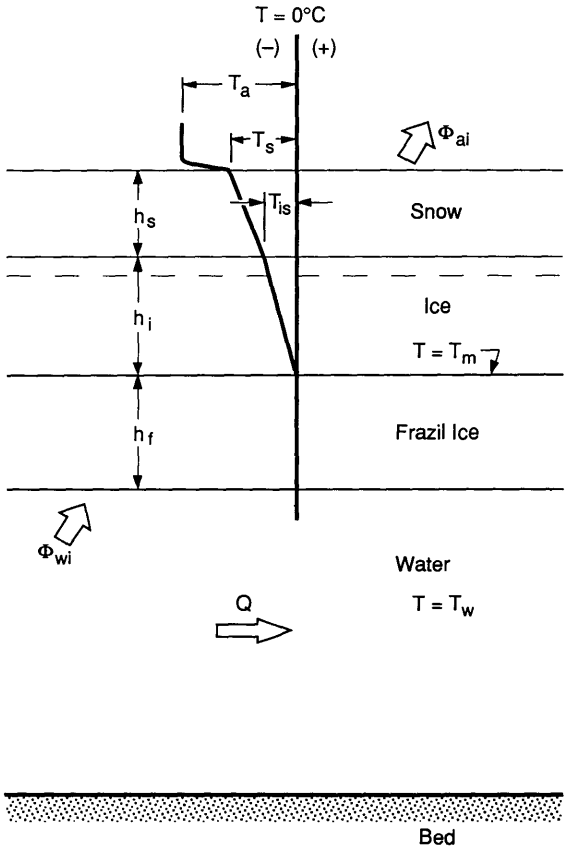

Figure 10. Definition sketch for ice cover growth.

$$h_f \leq h_{fo} + \frac{\rho_f}{\rho_w}\left(\frac{A_o}{B} - \frac{Q}{Bv_{ero}}\right). \tag{64}$$

Values of v_{dep} and v_{ero} have to be given as an input condition. When the water temperature is above freezing, the eroded frazil ice will first be melted by the heat of the water before bringing down the water temperature.

As a result of heat exchanges at the top and bottom surfaces, the ice cover will grow or decay during the winter. A finite-difference model developed by Shen and Lal (1986) is used in this study. In this model the following equation is used to calculate the rate of black ice growth at the bottom surface:

$$\rho_i L \frac{dh_i}{dt} = \frac{T_m - T_a}{\frac{1}{h_{wa}} + \frac{h_i}{k_i} + \frac{h_s}{k_s}} - h_{wi}\left(T_w - T_m\right) \tag{65}$$

where h_s and h_i = thicknesses of snow and solid ice
k_s and k_i = thermal conductivities of snow and ice
L = latent heat of fusion for ice (Fig. 10).

If frazil ice is present underneath the solid ice cover, solid ice growth will occur into the frazil ice layer, unaffected by turbulent heat exchange from the river flow. The rate of growth of solid ice, which is higher than without frazil ice accumulation, can be expressed as

$$e_f \rho_i L \frac{dh_i}{dt} = \frac{T_m - T_a}{\frac{1}{h_{wa}} + \frac{h_i}{k_i} + \frac{h_s}{k_s}} \tag{66}$$

where e_f is the porosity of the frazil ice. Similarly the rate of change of the frazil ice thickness can be expressed as

$$e_f \rho_i L \frac{dh_f}{dt} = - h_{wi}\left(T_w - T_m\right) - e_f \rho_i L \frac{dh_i}{dt}. \tag{67}$$

The ice growth rate in the absence of the snow layer can be determined by letting h_s equal 0.

Mechanical failure of an ice cover can take place at any time after the formation when the internal strength is not capable of withstanding the external forces. The condition for ice cover failure is

$$2\left(\tau_c t + \mu_1 f\right) < \left(\tau_i + \tau_g + \tau_a\right) B \tag{68}$$

where $f = \sigma_x^1 + \sigma_x^2 + \sigma_x^f$, and σ_x^1, σ_x^2 and σ_x^f are the longitudinal forces per unit width due to the solid ice, fragmented ice and frazil ice layers, respectively. When a section of ice cover fails, the fragmented ice masses will be transported downstream, where they will accumulate into a new ice cover when conditions permit.

SIMULATION OF OHIO RIVER ICE CONDITIONS

Study reach

The section of Ohio River simulated in this study extends from Pittsburgh, Pennsylvania (RM 981.80), to Meldahl Lock and Dam, Ohio (RM 545.40), with a total distance of 436.40 miles, as shown in Figure 11. In the numerical model the river system is schematized into segments connected at 186

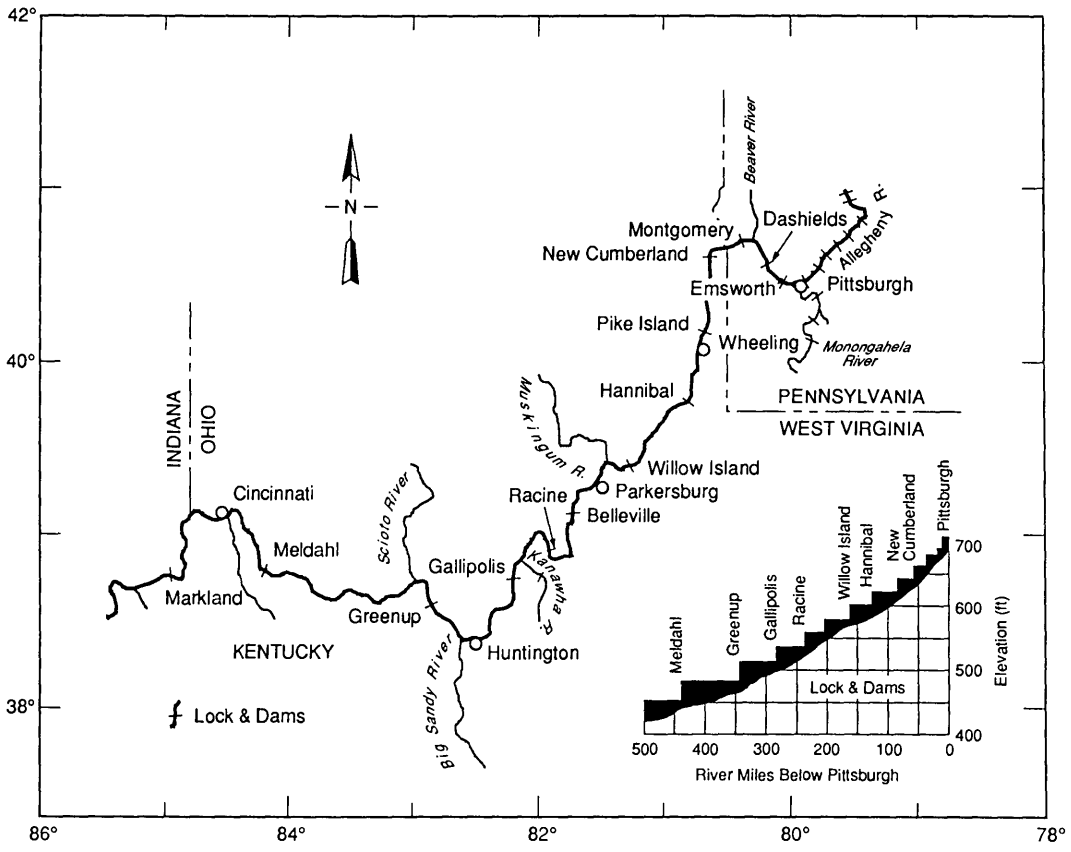

Figure 11. Ohio River between Pittsburgh and Meldahl L&D.

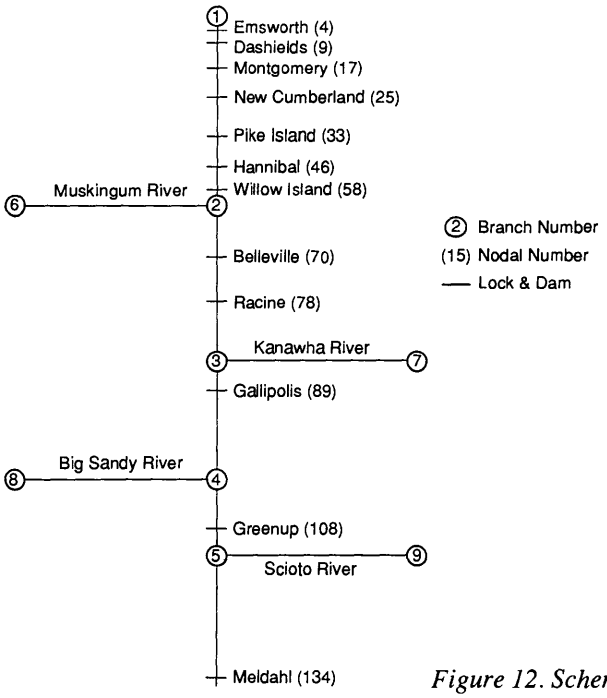

Figure 12. Schematization of the upper Ohio River system.

Table 1. Schematization of the Ohio River system.

Branch no.	Upstream nodal point	Downstream nodal point	Description
1	1	63	Ohio R. from Pittsburgh to Muskingum R.
2	64	85	Ohio R from Muskingum R. to Kanawha R.
3	86	100	Ohio R. from Kanawha R. to Big Sandy R.
4	101	111	Ohio R. from Big Sandy R. to Scioto R.
5	112	134	Ohio R. from Scioto R. to Meldahl L&D
6	135	148	Muskingum R.
7	149	162	Kanawha R.
8	163	171	Big Sandy R.
9	172	186	Scioto R.

Table 2. Gauged lateral inflow distribution.

Nodal point	Description of inflow
13	Beaver River
66	Little Kanawha River
69	Hocking River
96	Guyandot River
99	Twelve Pole Creek
106	Little Sandy River
111	Little Scioto River

Table 3. Locks and dams on the Ohio River system.

Lock and dam	Pool elevation (ft)	Upstream nodal point
Emsworth	710.0	4
Dashields	692.0	9
Montgomery	682.0	17
New Cumberland	664.5	25
Pike Island	644.0	33
Hannibal	623.0	46
Willow Island	602.0	58
Belleville	582.0	70
Racine	560.0	78
Gallipolis	538.0	89
Greenup	515.0	108
Meldahl	485.0	133
Winfield	566.0	154

nodal points, as shown in Figure 12. Some of the tributaries are treated as separate branches (Table 1), and others are treated as lateral inflows (Table 2). The entire system, which covers more than 600 miles, consists of 9 branches, 4 junctions and 13 navigation locks and dams (Table 3). The nodal points are irregularly spaced, with distances ranging from 1 to 5 miles, with closer spaces around locks and dams or junctions. Figure 13 shows the discharges of the Ohio River and its major tributaries for the 1985–86 winter, provided by the Ohio River Division of the U.S. Army Corps of Engineers. The geometric data tables required by the computer model RICEOH were constructed using data furnished by the Ohio River Division of the U.S. Army Corps of Engineers. The procedure for obtaining the geometrical data was fully explained by Johnson (1982).

Lateral inflows were furnished by the Ohio River Division as either gauged or ungauged data. The gauged flows represent flow from small rivers that are not treated as routed branches. The ungauged data are normally given as inflow to be distributed along relatively large reaches of the Ohio River. Based upon navigation maps showing natural drainage lines into the Ohio River, the distribution of ungauged lateral inflows presented in Table 4 has been prescribed by Johnson (1982).

Water and air temperature data are available at five locks and dams: Emsworth, Montgomery, Hannibal, Racine and Meldahl (Fig. 14). The air temperature data are linearly interpolated to each node in the system. The water temperature at the upstream boundary on the Ohio River is set to be 0°C when the air temperature is below freezing and water temperature measurements at Emsworth L&D are close

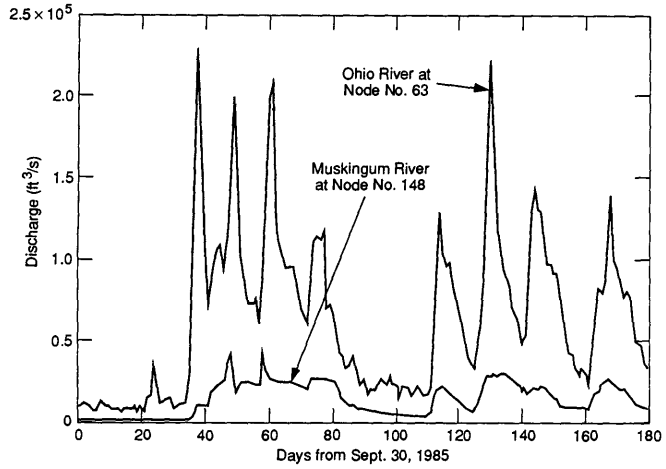

a. Discharges of the Ohio River at Node No. 63 and the Muskingham River at Node No. 148.

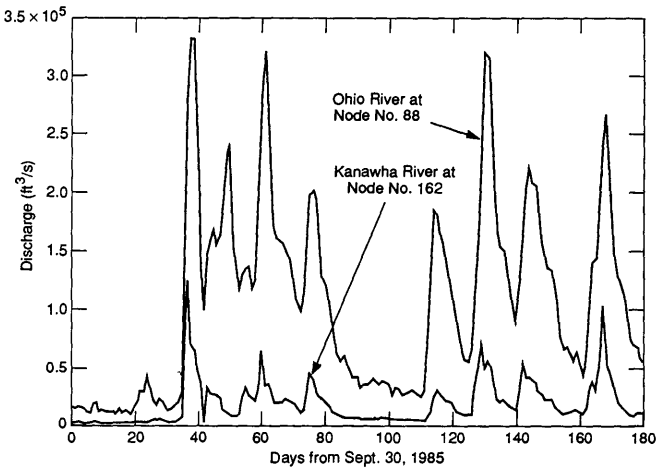

b. Discharges of the Ohio River at Node No. 88 and the Kanawha River at Node No. 162.

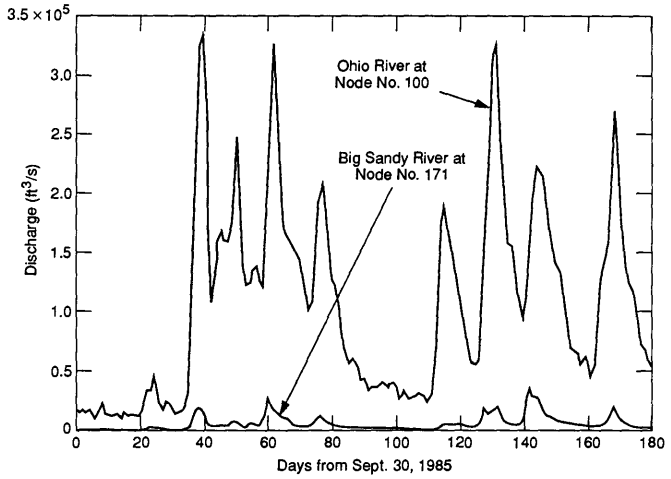

c. Discharges of the Ohio River at Node No. 100 and the Big Sandy River at Node No. 171.

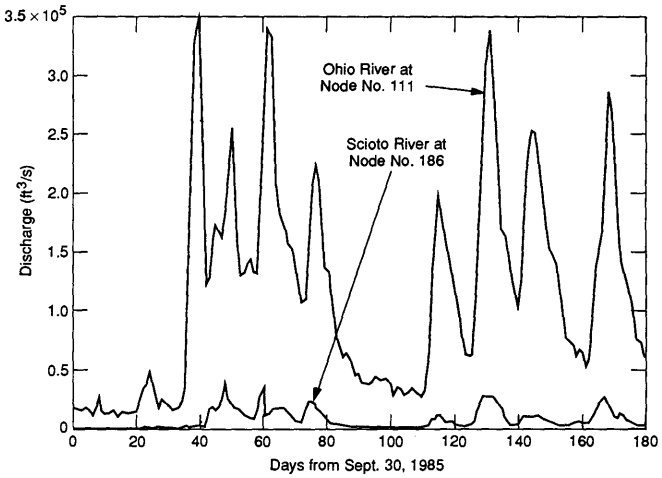

d. Discharges of the Ohio River at Node No. 111 and the Scioto River at Node No. 186.

Figure 13. Discharges of the Ohio River and its major tributaries for the 1985–86 winter.

to freezing; otherwise it was assumed to be the same as the water temperature at Emsworth L&D. Since no data were available for tributaries, the air temperature along the tributary is assumed to be the same as the air temperature at the junction of the tributary and the main stream. The water temperature at the upstream end of each tributary was set to be the same as the water temperature immediately upstream of the junction of the tributary and the main stream.

Numerical simulation and results

The computer model was applied to the upper Ohio River system for the 1985–86 winter. The first step in the simulation was to calibrate the heat exchange coefficient h_{wa}. The calibration was made based on the data at Montgomery and Hannibal using a least-squares technique (Lal 1988). These two stations were selected since there is no tributary inflow between them. This calibration gives h_{wa}=23.9 $Wm^{-2}°C^{-1}$. This value is applied to the entire study reach. The field data also indicate that the water

Table 4. Ungauged lateral inflow distribution.

Nodal point	*Ungauged reach*	*Percent of flow*	*Nodal point*	*Ungauged reach*	*Percent of flow*
3	Pittsburgh–Wheeling	5	81	Pomeroy–Huntington	20
8	Pittsburgh–Wheeling	5	83	Pomeroy–Huntington	10
10	Pittsburgh–Wheeling	5	84	Pomeroy–Huntington	10
13	Pittsburgh–Wheeling	5	87	Pomeroy–Huntington	10
16	Pittsburgh–Wheeling	7	91	Pomeroy–Huntington	20
20	Pittsburgh–Wheeling	13	97	Pomeroy–Huntington	30
24	Pittsburgh–Wheeling	13			100
28	Pittsburgh–Wheeling	17	105	Huntington–Maysville	30
32	Pittsburgh–Wheeling	30	114	Huntington–Maysville	10
		100	120	Huntington–Maysville	30
36	Wheeling–St. Mary	18	124	Huntington–Maysville	30
40	Wheeling–St. Mary	13			100
45	Wheeling–St. Mary	16	129	Maysville–Cincinnati	30
51	Wheeling–St. Mary	30	132	Maysville–Cincinnati	40
55	Wheeling–St. Mary	23	N/A	Maysville–Cincinnati	30
		100	100		
67	St. Mary–Pomeroy	10			
68	St. Mary–Pomeroy	10			
73	St. Mary–Pomeroy	30			
76	St. Mary–Pomeroy	20			
77	St. Mary–Pomeroy	10			
77	St. Mary–Pomeroy	20	100		

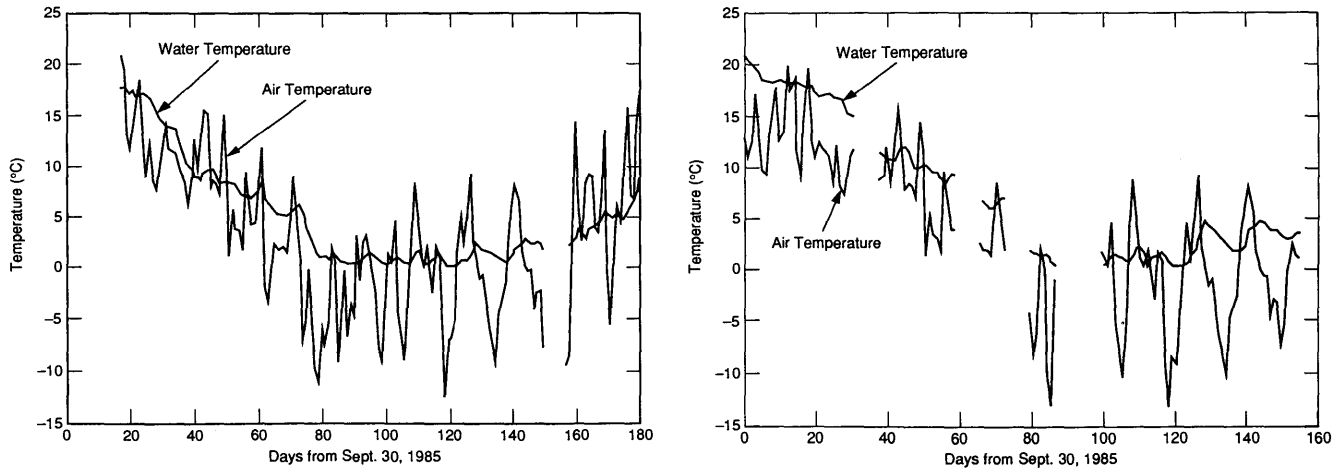

a. Emsworth L&D. *b. Montgomery L&D.*

Figure 14. Air and water temperatures at five locks and dams.

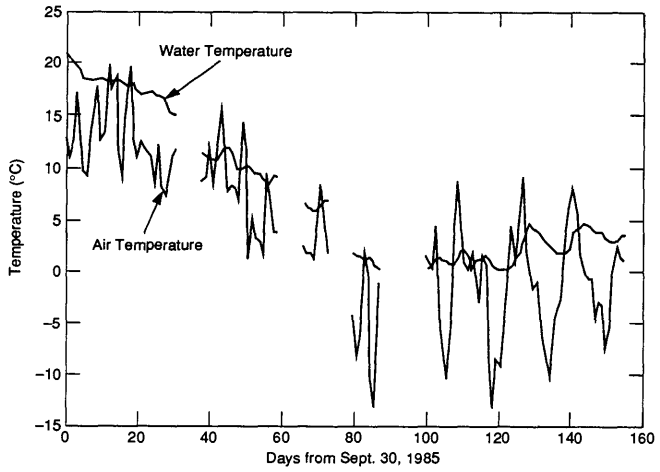

c. Hannibal L&D.

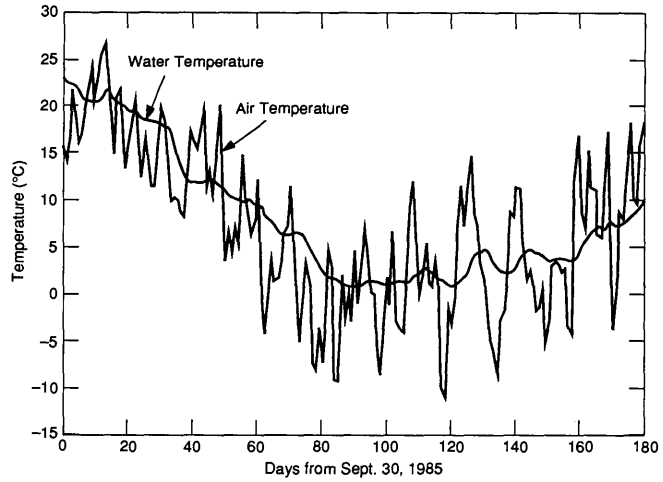

d. Racine L&D.

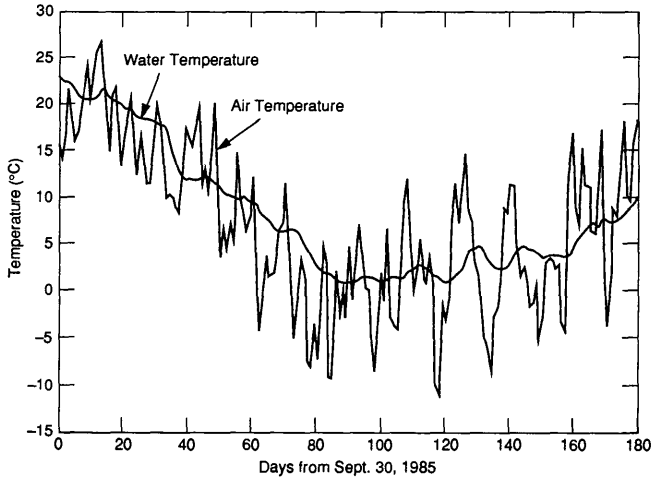

e. Meldahl L&D.

Figure 14 (cont'd). Air and water temperatures at five locks and dams.

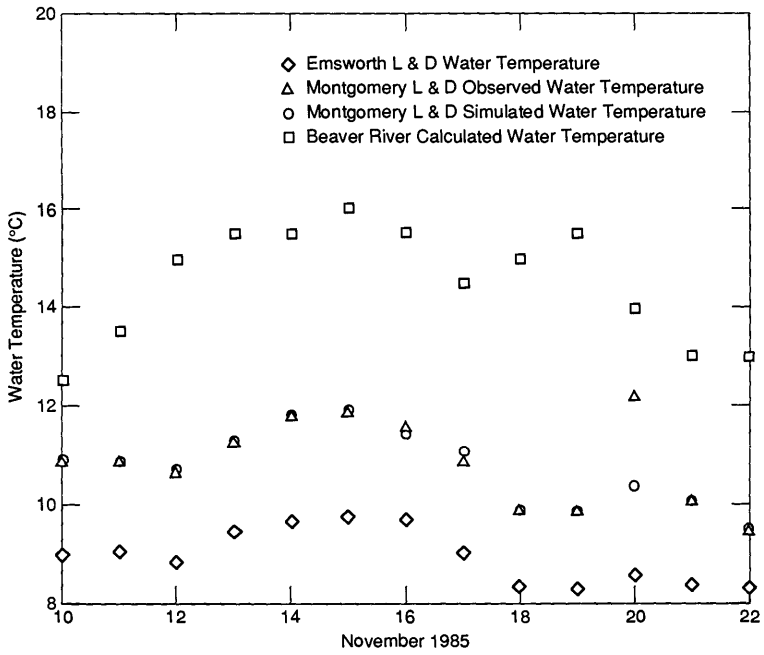

Figure 15. Comparison of the water temperatures at Emsworth L&D, Montgomery L&D and the Beaver River.

temperature at Montgomery is approximately 2°C higher than that of Emsworth, although Montgomery is only 25 miles downstream of Emsworth and the air temperatures at these two stations are about the same. This phenomenon can only be explained by considering thermal effluents discharged into the river by local industries. Since there is no record of the magnitude and distribution of thermal effluents, it is assumed that the effect of thermal effluents can be modeled by considering thermal effluent discharges into the Ohio River from the Beaver River. The validity of this assumption is substantiated by the existence of a large open-water area in the vicinity of the Beaver River and Ohio River confluence during the midwinter ice-covered period (Gatto et al. 1987). A calibration was then carried out to determine the water temperature of the Beaver River inflow. Figure 15 shows the calculated Beaver River water temperature and the measured and calibrated water temperatures at Montgomery and Emsworth. The temperature of the Beaver River inflow is approximately 4°C higher than the Ohio River temperature during the calibration period. This difference is expected to decrease during the winter. It is recommended that additional water temperature measurements be obtained at the downstream end of the Beaver River to be able to accurately account for the effect of thermal effluents in this reach. Figure 16 shows the comparison between the observed and simulated water temperatures at Hannibal, along with the observed water temperature at Emsworth. Similar comparisons for water temperatures at Racine and Meldahl L&D are shown in Figure 17.

To simulate ice cover conditions, several additional parameters are needed. These include the ice floe thickness, the underside roughness of the ice cover, the critical Froude numbers, the buoyant velocity and the fraction of the surface ice discharge that will be used to form the ice cover. The values of these parameters used in the simulation are summarized in Table 5. The upstream boundary discharges of the Ohio River and its tributaries during the simulation period are shown

Table 5. Parameter values for sample simulation.

Parameter	*Value*
h_{wa}	23.9 W m^{-2} °C^{-1}
t	0.08 m
n_i	0.015 or 0.020
$F_{r,c}$	0.06
$F_{r,max}$	0.09
v_{dep}	0.6 m/s
v_{ero}	0.7 m/s
αv_b	0.001 m/s
α_c	0.85
e_c	0.2
e_f	0.6
μ	0.28
τ_c	0.98 kPa

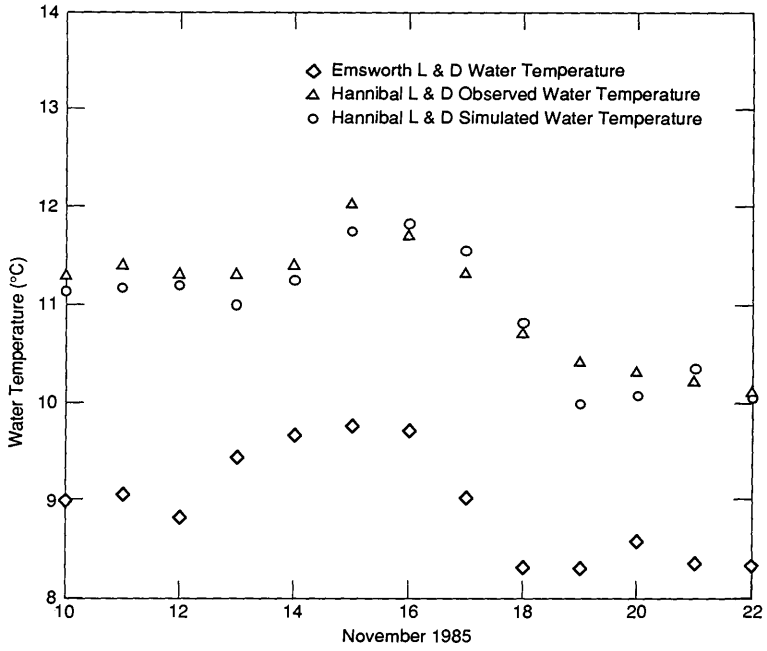

Figure 16. Comparison of the water temperatures at Emsworth L&D and Hannibal L&D.

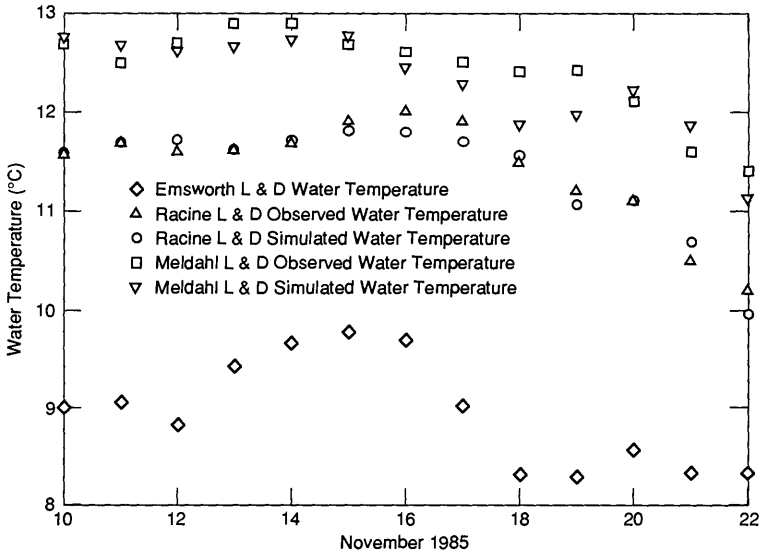

Figure 17. Comparison of the water temperatures at Emsworth L&D, Racine L&D and Meldahl L&D.

in Figure 18. The rating curve used at the downstream boundary (Node No. 134) was constructed from the data supplied by the Ohio River Division (Fig. 19). The underside roughness of an ice cover n_i can affect the energy slope and therefore the water levels. Since no observed water level data are available for the Ohio River, no calibration was made and the roughness coefficient n_i is assumed to be equal to 0.015 or 0.02.

The ice cover on the Ohio River is formed only by juxtaposition, and no narrow or wide jams were observed either in the field or in the simulated results. The thickness of the initial ice cover is the main

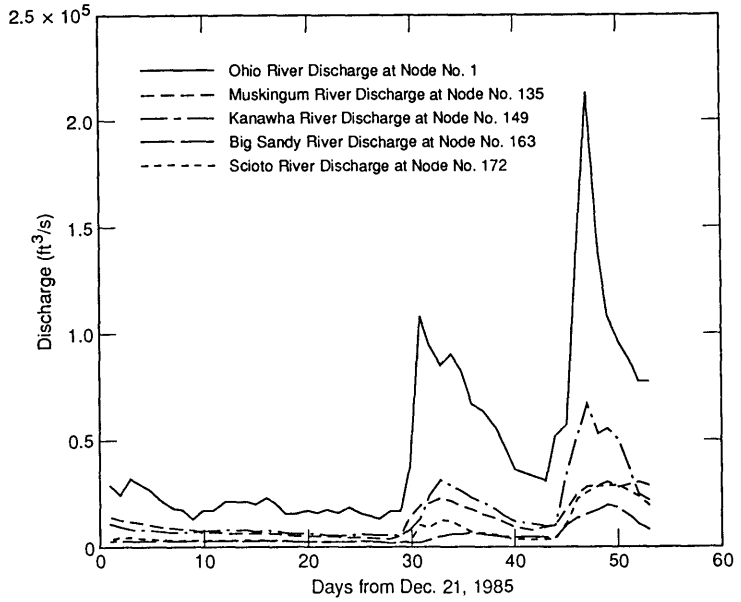

Figure 18. Discharges during the simulation period.

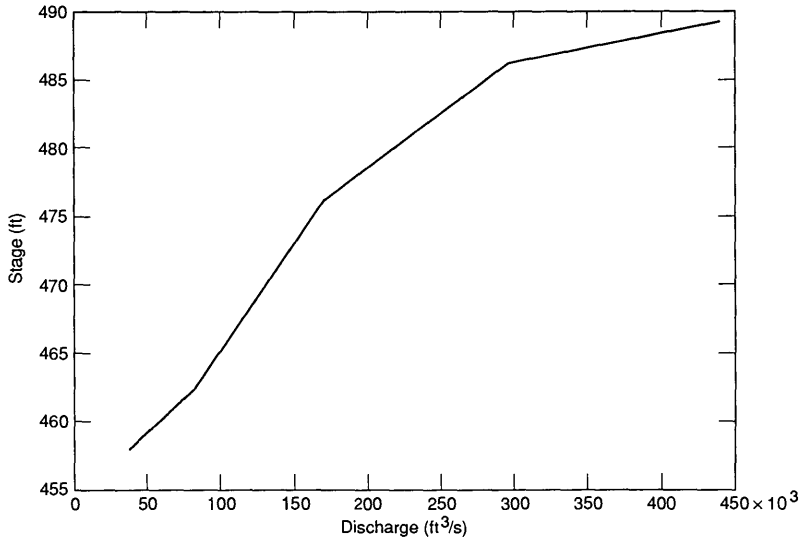

Figure 19. Rating curve at the downstream boundary.

parameter governing the rate of ice cover progression. In general, the ice cover progresses upstream very fast immediately after its initiation. During warm periods the cover can melt away completely without re-forming.

Two sets of data were available for comparison between the simulated and observed ice cover lengths. The ice atlas for the Ohio River 1985–86 season (Gatto et al. 1987) has a few days of observations during the winter when the river was covered with ice. The ice atlas was prepared from videotape records. In addition, navigation charts based on manual estimates of the lengths of ice covers from lock and dams were available. These data are less reliable and do not compare well with the ice atlas. The navigation chart data becomes inaccurate when the length of the ice cover was greater than the visible distance from the dam and smaller than the length of the pool. However, these charts provide

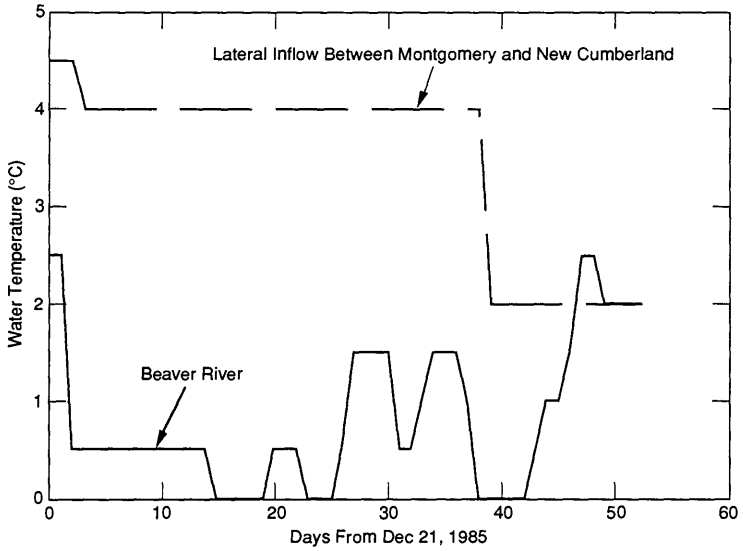

Figure 20. Temperatures of thermal inflows.

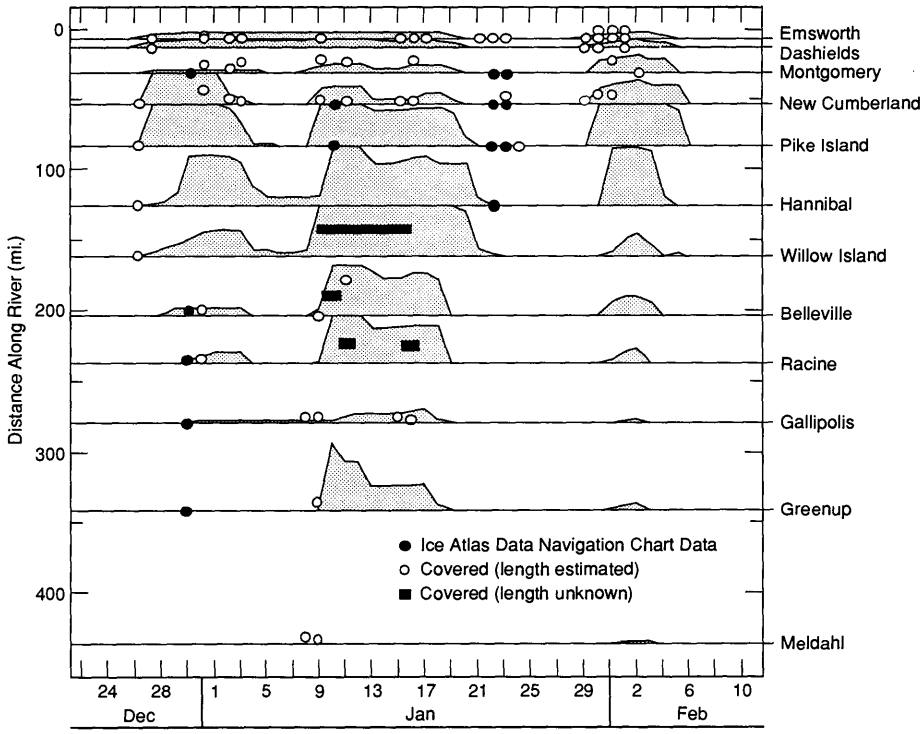

a. Ice cover roughness = 0.015 and one thermal lateral inflow.

Figure 21. Observed and simulated ice covers.

good information on the first appearance of the ice cover in each pool, and this information compares well with the simulation, as shown in Table 6.

Preliminary calibration runs show that there is a significant heat inflow between Montgomery and New Cumberland L&D. This influx of heat affects the length of the ice cover in the New Cumberland pool. In the simulation this heat influx is accounted for by increasing the water temperature of lateral inflows, as shown in Figure 20. Figure 21 shows the comparison of simulated and observed lengths

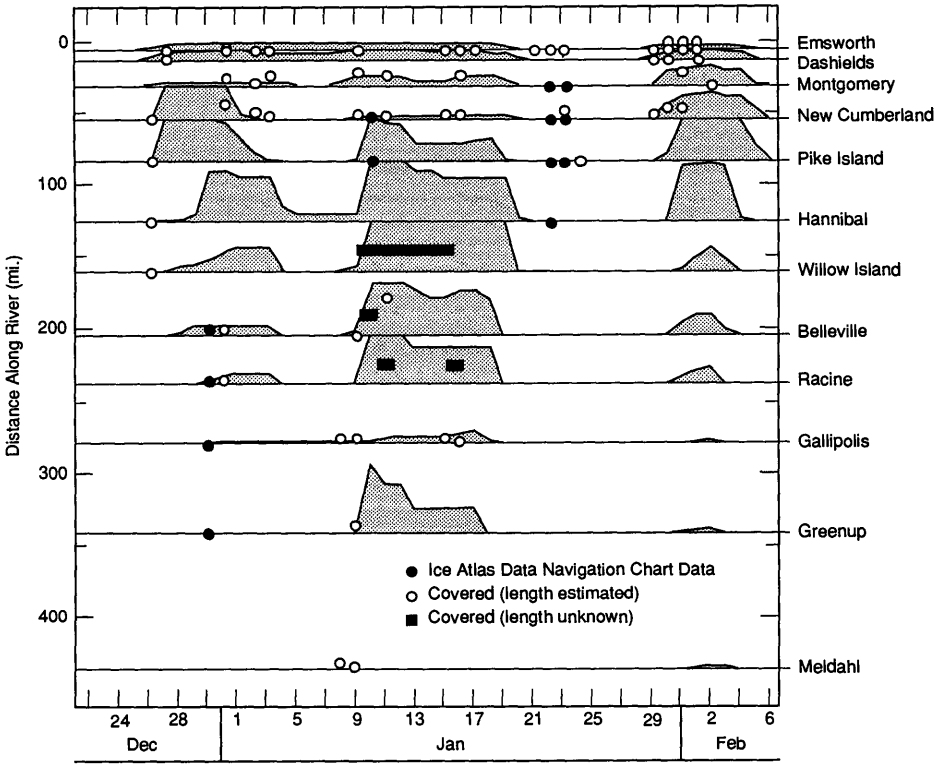

b. Ice cover roughness = 0.015 and two thermal lateral inflows.

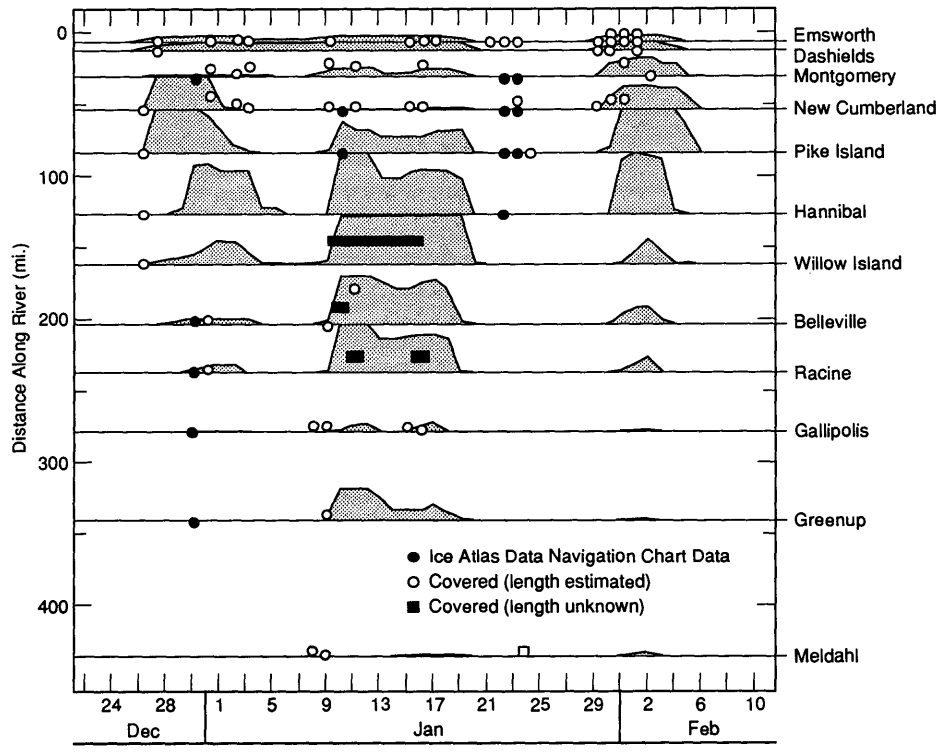

c. Ice cover roughness = 0.020 and two thermal lateral inflows.

Figure 21 (cont'd).

of ice covers in pools along the Ohio River. In Figure 21a a water temperature of 4°C was assigned to one of the lateral inflows between Montgomery and New Cumberland L&D. In Figures 21b and 21c the 4°C water temperature was assigned to both lateral inflows. Figures 21b and 21c show that the effect of n_i is relatively insignificant.

Table 6. First appearance of the ice cover.

Lock and dam	*Simulated*	*Observed*
Emsworth	12/26	12/27
Dashields	12/26	12/27
Montgomery	12/27	12/27
New Cumberland	12/27	12/26
Pike Island	12/27	12/26
Racine	12/28	12/27

SUMMARY AND CONCLUSION

The purpose of this study was to develop a model for simulating river ice and flow conditions. The model ORICE was developed and tested on the Ohio River system between Pittsburgh and Meldahl. Together with good weather forecasts and proper geometric data required by program, this model can be applied to any river system of dendritic configuration to forecast river ice conditions.

Field data on the Ohio River system are marginally adequate. Comparisons between the lengths of simulated and observed ice covers are given in Figure 21. We can conclude that the simulation compares very well with the ice atlas.

The information on the ice cover conditions from navigation charts and simulations compare very well in pools of the lower dams and those of Emsworth and Dashields. Slight discrepancies can be noticed in the Montgomery and New Cumberland pools. Significant differences between the ice atlas and the navigation charts are also found in these two reaches. This poses a reasonable doubt as to the accuracy of the information from the navigation charts. The accuracy of the simulation can be improved if more data on thermal discharges can be obtained. We believe that the thermal discharges that were assumed in this study are not the only ones on the Ohio River. Also, correct water temperatures at the upstream boundaries of tributaries, together with air temperature measurements, would provide information for more accurate simulation.

To calibrate the ice cover roughness accurately, it would be necessary to collect water stage data and compare these with the simulation. The present study, however, shows that ice cover progression is not very sensitive to variations in ice cover roughness n_i.

LITERATURE CITED

Ashton, G.D. (1974) Froude criterion for ice-block stability. *Journal of Glaciology,* **13** (68): 307–313.

Ashton, G.D. (1986) *River and Lake Ice Engineering.* Littleton, Colorado: Water Resources Publications.

Burden, R.L. and J.D. Faires (1986) *Numerical Analysis.* Third edition. Boston: Prindle, Weber and Schmidt Publishers.

Calkins, D.J. (1984) Numerical simulation of freeze-up on the Ottaquechee River. *Proceedings of the Third Workshop on the Hydraulics of River Ice, Fredericton, New Brunswick, Canada,* p. 247–277.

Chen, Y.H. and D.B. Simons (1975) Mathematical modeling of alluvial channels. *Symposium on Modeling Techniques: Second Annual Symposium of the Waterways, Harbors, and Coastal Engineering Division of ASCE, San Francisco, California.*

Daly, S.F. and K.D. Axelson (1990) Stability of floating and submerged blocks. *Journal of Hydraulic Research,* **28** (6): 737–752.

Gatto, L., S.F. Daly and K. Carey (1987) Ice atlas 85–86. USA Cold Regions Research and Engineering Laboratory, Special Report 87-20.

Johnson, B.H. (1982) Development of a numerical modeling capability for the computation of unsteady flow of the Ohio River and its major tributaries. USA Engineer Waterways Experiment Station, Vicksburg, Mississippi, Technical Report HL-82-20.
Kivisild, H.R. (1959) Hydrodynamical analysis of ice floods. *Eighth IAHR Congress, Montreal, Canada,* paper 23F.
Lal, A.M.W. (1988) A numerical model for river ice processes. Ph.D. dissertation, Clarkson University, Potsdam, New York.
Ligget, J.A. and J.A. Cunge (1975) Numerical methods of solution of the unsteady flow equations. In *Unsteady Flow in Open Channels* (K. Mahmood and V. Yenjevich, Ed.). Fort Collins, Colorado: Water Resources Publications.
Mahmood, K. and V. Yenjevich (Ed.) (1975) *Unsteady Flow in Open Channels.* Fort Collins, Colorado: Water Resources Publications.
Marcotte, N. (1981) Regime thermique et tegime des glaces en rivere: Etude de cas. *Proceedings, IAHR International Symposium on Ice, Quebec, Canada,* vol. 1, p. 412–422.
Michel, B. and M. Drouin (1981) Courbes de remous sous les converts de glace de la Grande Riviere. *Canadian Journal of Civil Engineering,* **8** (1): 351–363.
Petryk, S. (1981) Numerical modelling and predictability of ice regime in rivers. *Proceedings, IAHR International Symposium on Ice, Quebec, Canada,* vol. 1, p. 426–436.
Pariset, E. and R. Hausser (1961) Formation and evolution of the ice covers on rivers. *Engineering Institute of Canada, Transactions,* **5** (1): 41–49.
Shen, H.T. and P.D. Yapa (1984) Computer simulation on the ice cover formation in the upper St. Lawrence River. *Proceedings of the Third Workshop on the Hydraulics of River Ice, Fredericton, New Brunswick, Canada,* p. 227–246.
Shen, H.T. and A.M.W. Lal (1986) Growth and decay of river ice covers. *Proceedings, Cold Regions Hydrology Symposium, AWRA, Fairbanks,* p. 583–592.
Uzuner, M.S. and J.F. Kennedy (1976) Theoretical model of river ice jams. *Journal of the Hydraulics Division, ASCE,* **102** (HY9): 1365–1383.
Yapa, P.D. and H.T. Shen (1986) Unsteady flow simulation for an ice-covered reach. *Journal of Hydraulic Engineering,* **112** (11): 1036–1049.

APPENDIX A: COMPUTER PROGRAM AND USER'S MANUAL

The model RICEOH consists of two major parts: the unsteady flow computation and the water temperature and ice cover condition simulations. The unsteady flow computation is based on the model set up and tested by Johnson (1982). Minor changes are made to account for the ice cover effect. The water temperature and ice simulation model was based on the river ice model developed by Lal (1988). The model of Lal was originally developed for a single-channel river. Improvements are made in the present model to accommodate a dendritic system. In addition RICEOH can treat lateral thermal inflows. The program was written in Fortran77. Different ice processes are modeled separately in the form of independent modules that are convenient for future modifications. The flow chart, which outlines the computational steps, is given in Figure A1.

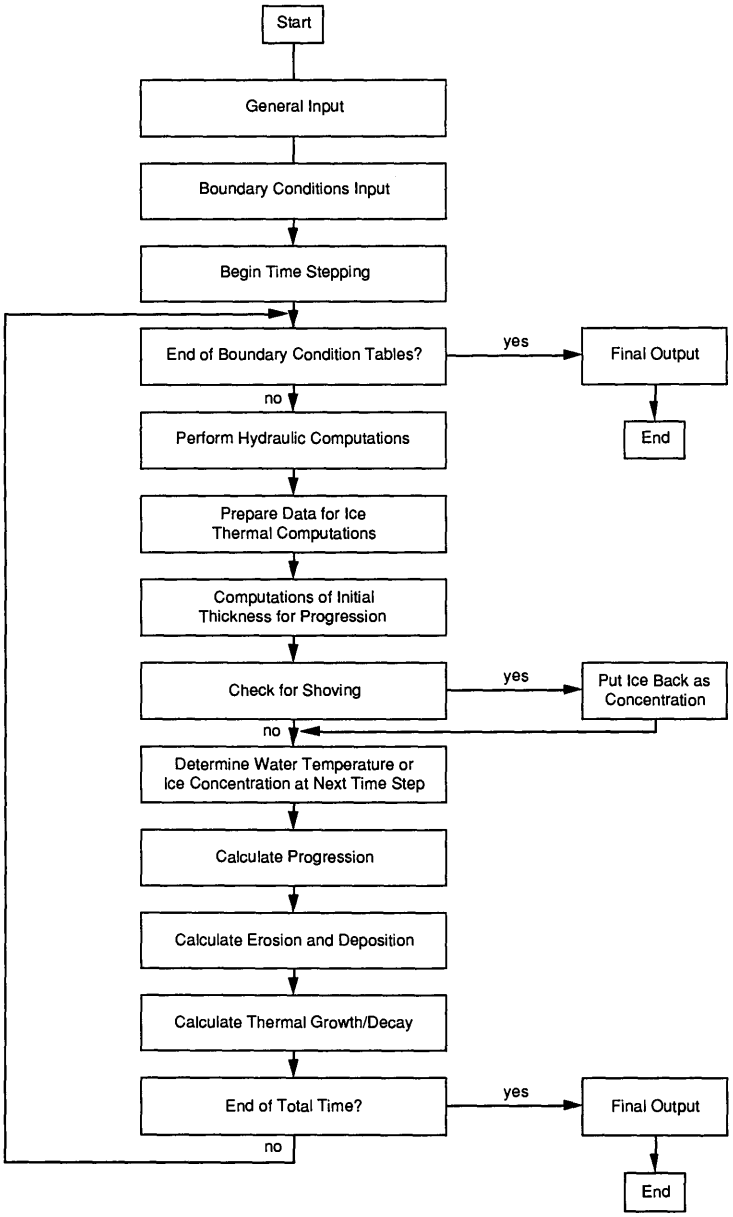

Figure A1. Flow chart of the computational steps in RICEOH.

Subroutine descriptions

The program is composed of a main program that controls the flow of computations and 30 subroutines that perform various functions. A brief description of the role of each subroutine is presented below. All of the subroutines from the original unsteady flow program (Johnson 1982) remain essentially the same.

LOCKDA sets coefficients in the equations applied to a computational reach containing a navigation lock and dam so that $Q_{us} = Q_{ds}$ and $y_{us} = f(t)$, where f is a known function of time.

LINEAR linearly interpolates values of the flow area, top width and Manning's roughness coefficient for a particular water surface elevation from geometric tables.

FLOOD determines the surface area of the flood plain used in computing the exchanges between the main channel and the flood plain $(q_l)_1$.

INITIA initializes the hydraulic computations. Various minor computations are performed, e.g. the flood plain area, which is input as a cross-sectional area and then changed to surface area, and the spatial computational steps are computed.

JOINTF joins the results from the forward sweep on the main river and a tributary with the confluence equations so that the forward sweep on the main river can continue.

COEFFI computes the coefficients in the system of linear algebraic equations (eq 24 and 25), which depend on information known from the previous time step. These coefficients are computed in this subroutine.

FORWAR computes the coefficients in the forward sweep of the double-sweep algorithm.

BACWAR computes the unknowns in the backward sweep of the double-sweep algorithm.

NEWFLO is called at the end of each time step to update flow conditions for initiating computations in the next time step.

DAMRC computes pool elevations upstream of the lock and dam from a rating curve at the structure.

DOWNCO computes difference coefficients. The rating curve at the downstream end of the main river is given in the form of a number of linear segments. Each linear segment is defined by specifying the discharge and corresponding elevation at the end of the segment. DOWNCO uses this information to compute the difference coefficients.

BRYCAL inputs time-dependent boundary data and returns either linearly interpolated data or the data that have just been read.

LATERA performs the same function as BRYCAL except that lateral inflows instead of open-boundary data are returned.

OPEN defines all input and output files.

REINT reads all information needed for thermal computations.

LAL links the main program and thermal computations.

PREPAR creates a separate subsystem for each branch of the river system. All computations will be performed on this subsystem.

POVRAT returns results of thermal computations from the subsystem to the main system.

ICE performs all ice-related computations by calling the subroutines for individual ice processes such as progression, erosion and growth.

AVERAG computes the reach-average values of geometrical and hydraulic variables from the known nodal values. This is required because all hydraulic computations are performed using variables defined at nodal points, while ice routines require reach-averaged variables.

NITHI computes the initial thickness of the ice cover for a given reach when the reach number is provided as a dummy argument. This subroutine has to be called once for each reach that has a leading edge and for which an initial ice thickness has to be computed. The initial thickness mainly depends on the hydraulics conditions of the reach, and in the process of determining it, juxtaposition, narrow

and wide jam modes are considered. Ice cover progression is limited by the maximum critical Froude number.

LAGRAN computes the distribution of water temperature or frazil ice concentration along the river. It uses a one-dimensional dispersion equation after neglecting the longitudinal dispersion term. A Lagrangian method is used to solve the equation. This method assumes that parcels of water having known temperatures are released from nodal points at the beginning of every time step. Their locations and concentrations are computed at the end of every time step. Nodal temperatures are determined from these values using linear interpolation.

OPENLA is called for each open water area. The results are stored separately to be used for the following reasons: a) When the subroutine LAGRAN is called, the final frazil concentration distribution is the sum of the convected ice and the ice generated in the open-water patches; b) When the volume of ice used for deposition or ice cover progression at a given reach is computed, frazil ice suspension, which has already completed the motion, is pulled back to add to the volume. OPENLA helps to sort out the amounts of ice created in different open-water reaches to make sure that any suspended portion of ice is deposited upstream from where it was produced.

PROGRE is called at every leading edge of the ice cover once during every time step. The current location of the leading edge has to be provided as a dummy argument. The subroutine computes the volume of ice that contributes to cover formation by taking a fraction of the ice discharge that has passed the leading edge. PROGRE computes all ice cover progressions that can take place at leading edges during the time step. Both the ice thickness and the horizontal extent of progression are computed. Changes in the local hydraulics are computed based on a backwater approximation.

OPLA uses the total amount of ice computed in LAGRAN to determine the amount of ice that can contribute to deposition. It separates the amounts of ice produced at open-water reaches downstream of the current reach because this ice cannot be deposited in any upstream reach. This separation is necessary because deposition or progression is computed as a reverse Lagrangian process or "pulling back" process.

TRAPEZ computes nodal values of ice concentration. During the computation of the ice cover progression and deposition, a portion of the moving ice is removed. Since concentrations are assigned to the nodes, the amount of ice removed from a reach takes a shape of a trapezoid in the longitudinal concentration profile. After removal of these trapezoidal shapes, the remaining concentrations have to be converted to nodal values before beginning of the next time step. Subroutine TRAPEZ computes these nodal values after conserving the mass and convection. This subroutine is called by PROGRE and ERODEP subroutines.

ERODEP computes the amount of erosion and deposition that takes place in a given reach. It is called once during every time step for every ice-covered reach in the river. The occurrence of erosion and deposition in a river reach is decided depending on the velocity of flow. In the computation of deposition, the total ice quantity that can be deposited is computed first. After depositing up to a critical limit, the excess ice is put back in the stream as concentration. Erosion is computed similarly, using a critical velocity criterion. Since the rate of erosion is not known, the eroded ice is distributed uniformly over the travel distance of a particle. If the water is warm, part or all of the ice cover can be melted.

SHOVE checks the stability of the ice cover against the net streamwise gravity and friction forces. The strength of the solid ice crust is considered in the computations. Parts of the initial ice cover and frazil deposited are considered as granular materials under passive stress conditions. If external forces are greater than the strength, the ice cover is assumed to fail in the current reach, as well as the upstream reaches downstream of the next ice control structure or ice bridge.

PUTBAC is called only if the ice cover in a given reach is known to fail as indicated by SHOVE. It first tries to re-form an initial ice cover using the fragments of broken cover. The formation conditions and the thickness of this initial cover are decided by the local hydraulic conditions. After

shoving, a new thicker ice cover can form, or the broken pieces can go under the cover and add to the ice discharge. This ice discharge travels downstream and can form a cover, be deposited under an existing cover or flush away through the downstream boundary. Subroutine PUTBAC is called once during every time step for every reach that is subjected to shoving.

GROWTH is capable of simulating the thermal growth and decay of an ice cover in a given river reach. It has to be called once during every time step for every river reach that is partially or fully covered with ice. The model uses a steady-state finite-difference method to compute incremental growth or decay during every time step. Heat exchanges at the top and bottom surfaces are computed using linearized models. The model can simulate both black and white ice growth while having a layer of snow on top and frazil ice at the bottom.

Input data

Input data for the model can be divided into two major groups, i.e. input data for hydraulic computations and input data for thermal-ice computations. Input data for the hydraulics part consist of four data files. FILE4.DAT contains general information about the system, such as the number of nodal points, the number and description of branches and joints and description of dams and lateral inflows. FILE2.DAT contains prescribed initial stages and discharges for every point of the system and discharges for dams that had a rating curve as input in FILE4.DAT. FILE5.DAT contains all geometrical information, such as cross-sectional area, top width, Manning's roughness coefficient and flood plain area, given as a function of stage for every point of the system. FILE1.DAT contains daily values of lateral inflows for every lateral inflow point, boundary discharges for every branch in the system, and elevations for all dams in the system that do not have a rating curve as input. These files are the same as files used in the unsteady flow model for the Ohio River (Johnson 1982) except that the system immediately downstream of Meldahl was not included.

Input data for thermal-ice computations are separated into two data files. FILE6.DAT contains general parameters used in thermal computations, including the density of water and ice or the water-to-air heat exchange coefficient, followed by general ice parameters for every point, namely, ice roughness, particle and critical velocities and ice bridging description. The boundary temperature conditions are also stored in this file. During each day of the simulation, air temperatures at points where this information is available are prescribed. This includes temperatures at five lock and dams and temperatures at the first upstream and last downstream points of each branch. Also, boundary water temperatures for every branch and lateral inflow that is important for thermal computations are stored in this file.

FILE3.DAT contains the initial temperatures for both air and water at every point of the system. Depending on whether an ice cover already exists in the system or not, it may provide descriptions of present ice conditions for every river reach. This includes the length of the ice cover, the thickness of the solid ice cover, the frazil deposition thickness, the submerged thickness and the initial ice cover thickness. Water temperatures in this file can be negative. However, this means that there is a frazil ice concentration at that point, and the water temperature is actually 0°C.

Detailed explanations of every input statement in the program and a sample of input data files follow. More information about input data for the hydraulic part of the program, as well as plotting capabilities, is provided by Johnson (1982).

Input statements

Statement 1
Variable: TITLE(I)
Format: 10A8
File read: FILE4

Variable	*Value*	*Meaning*
TITLE		Descriptive title of the run

Statement 2
Variables: IGEOM, ILUG, IPUNCH, IBACK
Format: 4I5
File read: FILE4

Variable	*Value*	*Meaning*
IGEOM	0	Geometry tables printed
	1	Geometry tables not printed
ILUG	90	File from which geometry tables are read
IPUNCH	$\neq 0$	Initial conditions not printed
IBACK	$\neq 0$	Less printed output

Statement 3
Variables: NC, NBRS, NJUNC, NDAMS, NXMAIN, ISTAGE, IFPLN, TOTALT, TSTEP
Format: 7I5, 10X, 2F10.0
File read: FILE4

Variable	*Value*	*Meaning*
NC	185	Total number of nodal points minus one
NBRS	9	Total number of branches
NJUNC	4	Total number of junctions
NDAM	13	Total number of dams
NXMAIN	134	Last nodal point on the main stream
ISTAGE	5	Number of entries in channel geometry tables
IFPLN	3	Number of entries in flood plain tables
TOTALT	2	Number of days of computation
TSTEP	3600	Time step in seconds

Statement 4
Variables: NSTAT, IPRINT, INTVG, INTVD, INTVP, NOXS
Format: 6I5
File read: FILE4

Variable	*Value*	*Meaning*
NSTAT	37	Number of nodal points at which output is requested
IPRINT	$\neq 0$	Detailed output provided
INTVG	24	Major print interval
INTVD	24	Small print interval for particular days (see following card)
INTVP	24	Interval for placing points in plot file
NOXS	0	Number of stations at which plots are desired

Statement 5
Variables: STDP, ISDDP, ISMDP, ISYDP, ETDP, IEDDP, IEMDP, IEYDP
Format: F10.0, 3I5, 5X, F10.0, 3I5
File read: FILE4

Variable	*Value*	*Meaning*
STDP		Starting time on 24-hr clock for small print interval
ISDDP		Starting day for small print interval
ISMDP		Starting month for small print interval
ISYDP		Starting year for small print interval
ETDP		Ending time on 24-hr clock for small print interval
IEDDP		Ending day for small print interval
IEMDP		Ending month for small print interval
IEYDP		Ending year for small print interval

If INTVD = INTVG, insert blank card for card 5.

Statement 6
Variables: NPRINT(I), I=1, NSTAT
Format: 16I5
File read: FILE4

Variable	*Value*	*Meaning*
NPRINT(I)		Nodal points at which output is desired

Statement 7
Variables: IPLT, ISCL, IYCN, IOP1
Format: 4I5
File read: FILE4

Variable	*Value*	*Meaning*
IPLT	0	No plots
	1	Elevation plots
	2	Discharge plots
	3	Elevation and discharge plots
	4	Velocity plots
	5	Elevation and velocity plots
	6	Discharge and velocity plots
	7	Elevation, discharge and velocity plots
ISCL	1440	Number of minutes/inch on x-axis
IYLN	0	Length of y axis in inches (0 defaults to 8 inches)
IOP1	0	Different y interval on each plot
	1	Same y interval on each plot

Statement 8
Variables: STITLE(I), NPLOT(I)
Format: A32, 3X, I5
File read: FILE4

Variable	*Value*	*Meaning*
STITLE(I)		Title of I^{th} station
NPLOT(I)		Nodal point number of I^{th} station

Statement 9
Variables: ID, IBRNCH(I,1), IBRNCH(I, 2), IBRS(I), IBC(I)
Format: 5I5
File read: FILE4

Variable	*Value*	*Meaning*
ID		Branch number
IBRNCH(I,1)		First nodal point of the branch
IBRNCH(I,2)		Last nodal point of the branch
IBRS(I)	1	Branch has upstream outer boundary
	0	Interior branch
	−1	Branch has downstream outer boundary
IBC(I)	−1	Rating curve will be used if this branch has downstream outer boundary
	0	This is an interior branch
	1	Elevations will be input if this branch has downstream outer boundary

There is one card no. 9 for each branch. All mainstream branches should be numbered before numbering tributaries.

Statement 10
Variables: ID, IJUNC(I,K), K=1,3, AL(J), AL(J+1)
Format: 4I5, 10X, 2F10.0
File read: FILE4

Variable	*Value*	*Meaning*
ID		Junction number
IJUNC(I,1)		Branch number of the main river upstream of the junction *I*
IJUNC(I,2)		Tributary branch number upstream of the junction *I*
IJUNC(I,3)		Branch number of the main river downstream of the junction *I*
AL(J)		Energy correction coefficients corresponding to node *I*

There is one card no. 10 for each junction.

Statement 11
Variables: TDAM(I), HSETO(I), NL(I), NVARY(I)
Format: A8, 2X, F10.0, 3I5
File read: FILE4

Variable	*Value*	*Meaning*
TDAM(I)		Name of the dam
HSETO(I)		Pool elevation maintained by dam
NL(I)		Nodal point immediately upstream of the dam
NVARY(I)	0	Pool elevation equal to HSETO(I)
	1	Time-varying elevations of pool are input
	2	Rating curve is input for I^{th} dam

Statement 12
Variables: IEDYHD
Format: I5
File read: FILE4

Variable	*Value*	*Meaning*
IEDYHD	0	Eddy head loss coefficients set to 0

If IEDYHD = 0, skip the following card.

Statement 13
Variables: N, CKE(N)
Format: I5, F10.2
File read: FILE4

Variable	*Value*	*Meaning*
N		Number of nodal point
CKE(N)		Eddy head loss coefficient for nodal point *N*

Card no. 12 is repeated IEDYHD times.

Statement 14
Variables: NRCH, (IRCH(I), I=1, NRCH)
Format: 16I5
File read: FILE4

Variable	*Value*	*Meaning*
NRCH	38	Total number of reaches containing lateral inflows
IRCH(I)		Numbers of the reaches containing lateral inflow

Statement 15
Variables: MNTH, KDAY, KYEAR, TIME
Format: 3I5, 5X, F10.0
File read: FILE2

Variable	*Value*	*Meaning*
MNTH	12	Starting month
KDAY	21	Starting day
KYEAR	86	Starting year
TIME	7	Starting time on a 24-hr clock

Statement 16
Variables: H(I,JSP), I=1, NX
Format: 8F10.0
File read: FILE2

Variable	*Value*	*Meaning*
H(I,JSP)		Initial water surface elevation in feet at each nodal point

Statement 17
Variables: Q(I,JSP), I=1, NX
Format: 8F10.0
File read: FILE2

Variable	*Value*	*Meaning*
Q(I,JSP)		Initial discharge in cfs at each nodal point

Statement 18
Variables: QL2L(K), K=1, NRCH
Format: 8F10.0
File read: FILE2

Variable	*Value*	*Meaning*
QL2L(K)		Initial lateral inflow discharge at all reaches containing lateral inflow

Statement 19
Variables: QCHECI(I)
Format: F10.0
File read: FILE2

Variable	*Value*	*Meaning*
QCHECI(I)		Initial discharge of dam that has a rating curve as input

There is one card no. 19 for every dam that has a rating curve as input.

Statement 20
Variables: NLEVEE, ILEVEE(I), I=1, NLEVEE
Format: 16I5
File read: FILE2

Variable	*Value*	*Meaning*
NLEVEE	0	Number of reaches with levees
ILEVEE(I)		Upstream nodal points of reaches with levees

Statement 21
Variables: ELEVEE(K), K=1, NLEVEE
Format: 8F10.0
File read: FILE4

Variable	*Value*	*Meaning*
ELEVEE(K)		Average elevation of the top of the levee along this reach in feet

If NLEVEE = 0, this card is skipped.

Statement 22
Variables: RANGE(I), XL(I), DUMMY, ZF(I), Z(I), BETA(I)
Format: A8, 2X, 7F10.0
File read: FILE5

Variable	*Value*	*Meaning*
RANGE(I)		Description of the I^{th} nodal point
XL(I)		River mileage of I^{th} nodal point
DUMMY		Space for top width; can be left blank
ZF(I)		Top bank elevation for I^{th} nodal point in feet
Z(I)		Bed elevation of I^{th} nodal point in feet
BETA(I)		Momentum correction factor

Statement 23
Variables: HI(I,J), AI(I,J), TI(I,J), RNI(I,J)
Format: 4F10.0
File read: FILE5

Variable	*Value*	*Meaning*
HI(I,J)		J^{th} elevation of channel geometry tables for point I
AI(I,J)		Flow area corresponding to elevation HI(I,J)
TI(I,J)		Top width corresponding to elevation HI(I,J)
RNI(I,J)		Manning's n corresponding to elevation HI(I,J)

Card no. 23 is repeated ISTAGE times.

Statement 24
Variables: HF(I,J), AFI(I,J), DUMMY, RNIFP(I,J)
Format: 4F10.0
File read: FILE5

Variable	*Value*	*Meaning*
HF(I,J)		J^{th} elevation of the channel flood plain geometry table
AFI(I,J)		Flow area corresponding to elevation HF(I,J)
DUMMY		Top width corresponding to elevation HF(I,J), can leave blank
RNIFP(I,J)		Manning's n corresponding to elevation HF(I,J)

Card no. 24 is repeated IFPLN times.
Cards no. 22, 23 and 24 are repeated for every nodal point.

Statement 25
Variables: NSEG
Format: I5
File read: FILE4

Variable	*Value*	*Meaning*
NSEG	6	Number of linear segments approximating the rating curve

Statement 26
Variables: QRC(I), HRC(I)
Format: 2F10.0
File read: FILE4

Variable	*Value*	*Meaning*
QRC(I)		Discharge at the end of the I^{th} linear segment
HRC(I)		Elevation of water surface corresponding to the end of the I^{th} segment

Card no. 26 is repeated NSEG times.

Statement 27
Variables: KRC(I), QLIMIT(I), QCHECKO(I), QDRCF(I), QDRC(K, I), HDRC(K,I), K=1, KRC(I)
Format: I5, 7F10.0/8F10.0
File read: FILE4

Variable	*Value*	*Meaning*
KRC(I)		Number of entries in rating curve table at the I^{th} dam
QLIMIT(I)		Discharge below which a fixed water surface elevation is prescribed
QCHECKO(I)		Initial discharge of the I^{th} dam
QDRCF(I)		Discharge above which the falling portion of the rating curve will be used if discharge is decreasing
QDRC(K,I)		K^{th} discharge in the rating curve table of dam I
HDRC(K,I)		Water surface elevation corresponding to QDRC(K,I)

Card no. 27 is repeated for each dam with NVARY(I) = 2.

Statement 28
Variables: J, QL2(K), K=1, NRCH
Format: I5, 7F10.0/8F10.0
File read: FILE1

Variable	*Value*	*Meaning*
J	24	Number of time steps before new lateral inflows will be input
QL2(K)		Lateral inflow in cfs

Statement 29
Variables: S, J
Format: F10.0, I5
File read: FILE1

Variable	*Value*	*Meaning*
S		New downstream boundary condition
J		Number of time steps before a new boundary condition will be input

Statement 30
Variables: GRAVIT, ROW, ROI, SPHT, XLATEN
Format: 5F10.0
File read: FILE6

Variable	*Value*	*Meaning*
GRAVIT	9.81	Acceleration of gravity in m/s^2
ROW	1000	Density of water in kg/m^3

ROI	916	Density of ice in kg/m^3
SPHT	4185.5	Specific heat of water
XLATEN	334000	Latent heat of melting of ice

Statement 31
Variables: ALPCOV, PORFRA, PORINI, VEROS, VDEPOS, VBUOY
Format: 6F10.0
File read: FILE6

Variable	*Value*	*Meaning*
ALPCOV	0.85	Fraction of concentration going for ice-cover formation
PORFRA	0.6	Porosity of frazil ice
PORINI	0.2	Porosity of initial ice cover
VEROS	0.6	Velocity of erosion in m/s
VDEPOS	0.5	Velocity of deposition in m/s
VBUOY	0.001	Buoyant velocity in m/s

Statement 32
Variables: XKS, XKI, ES, TOLNUL
Format: 4F10.0
File read: FILE6

Variable	*Value*	*Meaning*
XKS	0.25	Thermal conductivity of snow
XKI	2.24	Thermal conductivity of ice
ES	0.6	Porosity of snow
TOLNUL	0.00001	Small number used strictly for programming purposes

Statement 33
Variables: XMU, XK2, COHE, THIBLK, HWA, SIGMA
Format: 6F10.0
File read: FILE6

Variable	*Value*	*Meaning*
XMU	1.28	μ used in Pariset and Hausser's wide jam equation
XK2	3.0	Coefficient of passive stress for granular ice
COHE	100.0	Bank cohesion used in the wide jam equations
THIBLK	0.08	Initial thickness of ice block in m
HWA	23.9	Water to air heat transfer coefficient
SIGMA	81550	Compressive strength of solid ice crust formed due to cooling from top

Statement 34
Variables: LFTIM(IRCH(I)), I=1, NR
Format: 16I5
File read: FILE6

Variable	*Value*	*Meaning*
LFTIM(IRCH(I))	1	Lateral inflow will have temperature assigned
	0	Lateral inflow will not have temperature assigned

Statement 35
Variables: KDUM, IBOOM(I), DXICM(I), RICEM(I), FRPM(I), FRCM(I)
Format: 2I5, 4F10.0
File read: FILE6

Variable	*Value*	*Meaning*
KDUM		Number of the reach
IBOOM(I)	1	Ice bridging possible at the end of the reach
	0	Ice bridging not possible at the end of the reach
DXICM(I)		Initial length of the ice cover in reach *I*
RICEM(I)		Ice cover roughness on reach *I*
FRPM(I)	0.06	Critical Froude number for underturning
FRCM(I)	0.09	Critical Froude number for progression

Card no. 35 is repeated for every reach.

Statement 36
Variables: NXT
Format: I5
File read: FILE6

Variable	*Value*	*Meaning*
NXT	13	No. of nodal points where air temperature prescribed as boundary condition

Statement 37
Variables: NTA(I), I=1, NXT)
Format: 16I5
File read: FILE6

Variable	*Value*	*Meaning*
NTA(I)		Number of nodal point where air temperature is prescribed

Statement 38
Variables: NTW(I), I=1, NXTW
Format: 16I5
File read: FILE6

Variable	*Value*	*Meaning*
NTW(I)		Number of nodal point where water temperature is prescribed

Statement 39
Variables: IDUMM
Format: I5
File read: FILE3

Variable	*Value*	*Meaning*
IDUMM	0	No initial ice cover
	1	Existing initial ice cover

Blank card follows.

Statement 40
Variables: IDUM, DXICM(I), TICEM(I), TFRAM(I), TSUBM(I), THINIM(I)
Format: I5, 6F12.5
File read: FILE3

Variable	*Value*	*Meaning*
IDUM		Reach number
DXICM(I)		Ice cover length coefficient on reach *I*
TICEM(I)		Solid ice cover thickness in reach *I* in m
TFRAM(I)		Frazil ice thickness in reach *I* in m
TSUBM(I)		Submerged ice cover thickness in reach *I* in m
THINIM(I)		Initial ice cover thickness in reach *I* in m

There is one card no. 39 for every reach.
If IDUMM = 0 (card no. 38), there will be no card no. 39.
A blank card follows.

Statement 41
Variables: TWS(I), I=1, NX
Format: 10F7.0
File read: FILE3

Variable	*Value*	*Meaning*
TWS(I)		Initial water temperature at every nodal point

Two blank cards follow.

Statement 42
Variables: TAS(I), I=1, NX
Format: 10F7.0
File read: FILE3

Variable	*Value*	*Meaning*
TAS(I)		Initial air temperature at every nodal point

There is one blank card before card no. 41.

Statement 43
Variables: TWXA(I), I=1, NJUNC+1
Format: 8F10.0
File read: FILE6

Variable	*Value*	*Meaning*
TWXA(I)		Boundary water temperature at the upstream end of I^{th} tributary

Statement 44
Variables: TLIM
Format: F10.0
File read: FILE6

Variable	*Value*	*Meaning*
TLIM(I)		Temperature of the lateral inflow

Card no. 43. is repeated for every lateral inflow that had LFTIM(I) $\neq$ 0.

Statement 45
Variables: TAS(NTA(I)), I=1, NXT
Format: 8F10.0
File read: FILE6

Variable	*Value*	*Meaning*
TAS(NTA(I))		New boundary air temperature at point NTA(I)

Cards no. 44, 42 and 43 are repeated for every day of computation.

Output

Only printed output can be obtained as a result of the program. Several plotting programs are available to represent these results in graphic mode when needed. RES1.DAT contains all important parameters and descriptions of the system, followed by the time history of the water surface elevation, flow discharge and velocity, and bed elevation at each nodal point requested. RES2.DAT contains the time history of the water surface elevation and flow discharges for all nodal points, the lateral inflows and the discharges for dams with rating curves as input. This file can be used as input FILE2.DAT without any changes. RES3.DAT indicates whether the run was successful or not. RES4.DAT contains water and air temperatures for every nodal point along the river, followed by ice cover conditions. These include the reach number, the fraction of reach under an ice cover, the thickness of the solid ice cover, the thickness of frazil deposition, and the submerged and initial ice cover thickness. All thickness data are given in meters. If an ice cover is not present on the river, information about ice cover conditions is omitted. This file can be used as input FILE3.DAT.

Files RES1.DAT, RES2.DAT and RES3.DAT are exactly the same as the output files from the original hydraulics model, so they will not be discussed further. Detailed descriptions of these files are provided by Johnson (1982). A sample output of file RES4.DAT is given on the following pages. Since the results of the computations are given for each reach separately, it is not easy to interpret them for every pool. A small FORTRAN program is provided to rearrange these data in a simpler pattern. The listing of this program, together with its output, is given after the sample of output file RES4.DAT.

Limitations

RICEOH is a one-dimensional unsteady-flow thermal and ice model that can be applied to a general system of river channels containing locks and dams. However, there are some limitations to its applicability. This model can be applied only to a simply connected system, i.e. closed loops within the system cannot be handled. An additional limitation on the physical system is that there can be only one downstream boundary.

In its present form, there is some limitation on the specification of boundary conditions. At an upstream boundary, only flow discharges can be prescribed; at a downstream boundary, either a rating curve or water surface elevations may be specified. In general, one can specify elevations at the upstream boundary and discharges at the downstream boundary, but some additional modifications on the current version will be required.

The major limitation on the thermal and ice routines is that negative velocities cannot be handled. If any of the branches at any time flow upstream, the temperature computation cannot be performed. Since the time period of this simulation is mainly in the winter (the low-flow season), this limitation is not important.

Variable names

In this section definitions of input as well as other variables in the program are tabulated in Tables A1 and A2.

Table A1. Definitions and typical values of input variables.

Variable	*Value*	*Definition*
AI(i,j)		Cross-sectional area at elevation *HI(i,j)* (ft^2); *i* = 1, 2,...*NX*; *j* = 1, 2,...*ISTAGE*.
AFI(i,j)		Cross-sectional area of the flood plain at elevation; *HF(i, j)* (ft^2); *i* = 1, 2,...*NX*; *j* = 1, 2,...*IFPLN*.
AL(i)	1.0	Velocity head correction factor associated with junction of upstream main river and downstream main river; *I* = 1, 3,...*NJUNC* * 21.
AL(i)	1.0	Velocity head correction factor associated with junction of tributary and downstream main river; *I* = 2, 4,...*NJUNC* * 2–1.
ALPCOV	0.90	Fraction of total ice flow going into cover formation (0–1).
BETA(i)	1.0	Correction factor in momentum equation; *i* = 1, 2,...*NX*.
COHE	100.0	Bank cohesion used in the wide jam equations (kg m^{-2}).
DXICM(i)		Fraction of the length of a river reach covered by ice (0.0–1.0); *i* = 1, 2,...*NR*. Before the formation of ice cover, as input, set this variable to *TOLNUL* at all points where ice cover progression is possible.
DUM		Dummy variable.
ELEVEE(i)		Average elevation of the top of the levee along reach *i*; *i* = 1, 2,...*NLEVEE* (ft).
ES	0.6	Porosity of snow (0.0–1.0).
FRCM(i)		Critical Froude number above which ice cover progression is not possible in reach *i*; *i* = 1, 2,...*NX*.
FRPM(i)		Froude number below which particle juxtraposition takes place in the river reach *i*; *i* = 1, 2,...*NX*.
G	32.1614	Gravitational acceleration (ft s^{-2}).
GRAVIT	9.8	Gravitational acceleration (m s^{-2}).
H(i,1)		Initial water surface elevation at each net point (ft); *i* = 1, 2,...*NX*.
HDRC(j,i)		Water-surface elevation corresponding to *QDRC(j,i)* (ft); *j* = 1, 2,...*KRC(i)*.
HF(i,j)		Elevation of the flood plain geometry (ft); *i* = 1, 2,...*NX*; *j* = 1, 2,...*IFPLN*.
HI(i,j)		Elevation of channel geometry table *i* = 1, 2,...*NX*; *j* = 1, 2,...ISTAGE.
HRC(i)		Elevation of water surface corresponding to the end of the linear segment *i* (ft); *i* = 1, 2,...*NSEG*.
HSETO(i)		Elevation maintained by dam (ft).
HWA	23.9	Water-to-air heat transfer coefficient (W m^{-2} $°C^{-1}$).
IBACK	1	Normal output (if *IBACK* = 0 less printed output).
IBOOM(i)		Flag to indicate the presence of an ice boom, dam or ice control structure at the end of reach *i*. If = 1, ice cover can progress starting from the downstream end of reach *i*; *i* = 1, 2,...*NX*.
IBC(i)	–1	Rating curve will be used if this branch contains an outer downstream boundary.
	0	This is an interior branch, or discharge is input at its upstream boundary.
	1	Elevations will be input if this branch contains an outer downstream boundary.

Table A1 (cont'd).

Variable	*Value*	*Definition*
IBRNCH(*i*,1)		First net point on branch.
IBRNCH(*i*,2)		Last net point on branch.
IBRS(*i*)	0	Branch is an interior branch.
	1	Branch has an upstream outer boundary.
ID		Dummy argument.
IEDYHD	0	Eddy head loss coefficients set to zero (if *IEDYHD* = 1, eddy head loss coefficients are read in).
IFPLN	3	Number of entries in flood plain tables.
IGEOM	1	Geometry tables will not be printed (if *IGEOM* = 0, they will be printed).
IHSET	24	Number of time steps before a new water surface elevation to be maintained by dam is read.
IJUNC(*i*,1)		Number of upstream branch on main river before junction $i = 1, 2, \ldots NJUNC$.
IJUNC(*i*,2)		Number of tributary branch $i = 1, 2, \ldots NJUNC$.
IJUNC(*i*,3)		Number of downstream branch on main river after junction $i = 1, 2, \ldots NJUNC$.
ILEVEE(*i*)		Upstream net points of reaches with levees.
ILUG	90	Unit from which geometry tables will be read.
INTVD	24	Print interval for particular days.
INTVG	24	Major print interval.
INTVP	24	Interval for placing points in plot file.
IPLT	0	No plots.
IPRINT	0	Limited output (if *IPRINT* = 1, detailed output).
IQCK	24	Number of time steps before a new discharge will be input.
IRCH(*i*)		Numbers of the reaches containing lateral inflow $i = 1, 2, \ldots NRCH$.
ISTAGE	5	Number of entries in channel geometry tables.
J	24	Number of time steps before new lateral inflows will be input.
KRC(*i*)	15	Number of entries in rating curve table at the dam *i*.
LFTIM(*i*)		Indicator of thermal importance of lateral inflow; if *LFTIM*(*i*) = 1, lateral inflow *i* is thermal inflow.
NBRS	9	Total number of branches.
NC	185	Total number of net points minus one.
NDAMS	13	Total number of dams.
NJUNC	4	Total number of junctions.
NL(*i*)		Net point immediately upstream of dam.
NLEVEE	0	Upstream net points of reaches with levees.
NOXS	0	Number of stations at which plots are desired.
NPRINT(*i*)		Net point numbers at which output is desired; $i = 1, 2, \ldots NSTAT$.
NRCH	38	Total number of reaches containing lateral inflows.
NSEG	6	Number of linear segments approximating the rating curve.
NSTAT	37	Number of net points at which output is desired.
NTA(*i*)		Net point where boundary air temperature is prescribed.
NTILF	1	Number of lateral inflows that are thermal inflows.
NVARY(*i*)	0	Normal dam.

Table A1 (cont'd). Definitions and typical values of input variables.

Variable	*Value*	*Definition*
	1	Time-varying elevations of pool will be input.
	2	Rating curve will be input for this dam.
NXMAIN	134	Last net point on main river.
NXT	13	Total number of points where boundary air temperature is prescribed.
PORFRA	0.4	Porosity of frazil ice accumulation (0.0–1.0).
PORINI	0.2	Porosity of initial ice cover (0.0–1.0).
Q(*i*,1)		Initial discharge at each net point ($ft^3\ s^{-1}$); $i = 1, 2,...NX$.
Q(*i*,2)		New boundary discharge at upstream end of tributaries and main stream ($ft^3\ s^{-1}$).
QCHECO(*i*)		Initial discharge of dam *i* ($ft^3\ s^{-1}$).
QDRCF(*i*)		Discharge above which the falling portion of the rating curve for dam *i* will be used ($ft^3\ s^{-1}$).
QDRC(*j*,*i*)		Discharge in the rating curve table for dam *i* ($ft^3\ s^{-1}$); $j = 1, 2,...KRC(i)$.
QL2(*i*)		Lateral inflow ($ft^3\ s^{-1}$); $i = 1, 2,...NRCH$.
QLIMIT(*i*)		Discharge below which a fixed water-surface elevation for dam *i* is prescribed ($ft^3\ s^{-1}$).
QRC(*i*)		Discharge at the end of the linear segment *i* ($ft^3\ s^{-1}$); $i = 1, 2,...NSEG$.
RANGE(*i*)		Description of net point *i*; $i = 1, 2,...NX$.
RICEM(*i*)		Ice roughness for reach *i*; $i = 1, 2,...NX$.
RNI(*i*)		Manning's roughness coefficient at the elevation *HI*(*i*,*j*); $i = 1, 2,...NX$; $j = 1, 2,..., ISTAGE$.
RNIFP(*i*)		Manning's roughness coefficient at the elevation *HF*(*i*,*j*), $i = 1, 2,..., NX$, j = 1, 2,...*IFPLN*.
ROI	916.0	Density of ice ($kg\ m^{-3}$).
ROW	1000.0	Density of water ($kg\ m^{-3}$).
SIGMA	0.408×10^5	Compressive strength of solid ice crust formed due to cooling from top ($kg\ m^{-3}$).
SPHT	4.1855×10^3	Specific heat of water ($J\ kg^{-1}\ °C^{-1}$).
TAS(*i*)		Air temperature at net point *i* (°C); $i = 1, 2,...NX$.
TDAM(*i*)		Description of the dam.
TFRAM(*i*)		Thickness of frazil deposition on reach *i* (m); $i = 1, 2,...NX$; will be input only if *IDUMM* = 1.
THIBLK	0.08	Thickness of a floating ice floe (m).
THINIM(*i*)		Thickness of initial ice cover on reach *i* (m); i = 1, 2,...*NX*; will be input only if *IDUMM* = 1.
TI(*i*,*j*)		Top width in geometry table $i = 1, 2,...NX$; $j = 1, 2,...ISTAGE$.
TITLE		Description of run.
TICEM(*i*)		Thickness of solid ice cover on reach *i*; $i = 1, 2,...NX$; will be input only if *IDUMM* = 1 (m).
TLIM(*i*)		Water temperature of lateral inflow that has *LFTIM*(*i*) = 1 (°C).
TOLNUL	0.00001	Very small positive non-zero number used in programming.
TOTALT		Number of days of computations.

Table A1 (cont'd).

Variable	*Value*	*Definition*
TSTEP	3600	Time step (s).
TSUBM(i)		Thickness of submerged ice cover on reach *i* (m); *i* = 1, 2,...*NX*; will be input only if *IDUMM* = 1.
TT	86400.0	Length of time step used in the simulation (s).
TWS(i)		Initial water temperature at net point *i* (°C); *i* = 1, 2,...*NX*.
VBUOY	0.001	Buoyancy velocity of frazil ice particles used in determining the amount of deposition (m s^{-1}).
VDEPOS	0.6	Velocity of deposition, which is the velocity below which deposition of frazil ice under the ice cover is possible (m s^{-1}).
VEROS	0.7	Velocity of erosion, which is the velocity above which erosion of frazil ice under the ice cover is possible (m s^{-1}).
XKI	2.24	Thermal conductivity of ice (W m^{-1} $°C^{-1}$).
XKS	0.25	Thermal conductivity of snow (W m^{-1} $°C^{-1}$).
XK2	3.00	Coefficient of passive stress for granular ice; $XK_2 = \tan^2(\pi/4 + \phi/2)$.
XL(i)		River mileage of net point *i*; *i* = 1, 2,...*NX*.; tributary mileage is zero at junction (miles).
XLATEN	3.34×10^5	Latent heat of melting of ice (J kg^{-1}).
XMU	1.28	μ used in Pariset and Hausser's wide jam equation.
ZF(i)		Top bank elevation for net point *i* (ft); *i* = 1, 2,...*NR*.
Z(i)		Bed elevation for net point *i* (ft); *i* = 1, 2,...*NR*.

Table A2. Definitions of variables other than input variables used in the program.

Variable	*Definition*
A(i,1)	Flow area as calculated in hydraulic part during the current time step (ft^2); *i* = 1, 2,...*NX*.
A(i,2)	Flow area as calculated in hydraulic part during the previous time step (ft^2); *i* = 1, 2,...*NX*.
AB(i)	Average effective flow area of reach *i*. This area is used in water temperature and ice computations (m^2); *i* = 1, 2,...*NR*.
AD(i)	Downstream effective flow area of reach *i*; *i* = 1, 2,...*NR* (m^2).
AF(i)	Flood plain area as calculated in hydraulic part (ft^2); *i* = 1, 2,...*NX*.
AU(i)	Upstream effective flow area of reach *i*; *i* = 1, 2,...*NR* (m^2).
AXY(i,1)	Derivative of flow area along the channel when flow depth is kept constant during the current time step; *i* = 1, 2,...*NX*.
AXY(i,2)	Derivative of flow area along the channel when flow depth is kept constant during the previous time step; *i* = 1, 2,...*NX*.
BMAN(i)	Manning's roughness coefficient for reach *i*; *i* = 1, 2,...*NR*.
CO(i,j)	Coefficients of the two governing equations; *i* = 1, 2,...*NX**2; *j* = 1, 2, 3, 4.
CSI	Parts of *CO(i,j)*; *I* = 1, 2,...13.
E(i)	Right side coefficients of the two governing equations; *i* = 1, 2,...*NX**2.
FRCONV	Factor to convert temperature to ice concentration.

Table A2. Definitions of variables other than input variables used in the program.

Variable	*Definition*
IOAREA(i,j)	Variable to designate the extent of open-water patches in an ice-covered river; j = counter for the open water are starting from upstream ($\leq NR$); $i = 1$ gives the starting node number for j^{th} open water area; $i = 2$ gives the ending node number of j^{th} open water area; $i = 3$ gives the last node up to which a particle in this open-water area will travel during the time step.
D(i,1)	Depth of the flow in net point i during the current time step (ft); $i = 1, 2, \ldots NX$.
D(i,2)	Depth of the flow in net point i during the previous time step (ft); $i = 1, 2, \ldots NX$.
DHH	Value of δH used when calculating derivatives of geometric values with respect to the stage (ft).
DHT	Twice the value of *DHH*, used in calculating derivatives of geometric values with respect to the stage (ft).
DXIC(i)	Fraction of the length of a river reach covered by ice; $i = 1, 2, \ldots NR$.
HHD(i)	Downstream water level of reach i (m); $i = 1, 2, \ldots NR$.
HHU(i)	Upstream water level of reach i (m); $i = 1, 2, \ldots NR$.
IBOO(i)	Flag to indicate the presence of an ice boom, dam or an ice control structure at the end of the reach i; $i = 1, 2, \ldots NR$.
IPROG(i)	Flag to indicate whether progression is possible at reach i after checking jam conditions; 0 = no; 1 = yes; $i = 1, 2, \ldots NR$.
JEP	Variable used in controlling the time step.
JSP	Variable used in controlling the time step.
NB	Number of nodal points in branch while performing thermal computations.
NOAREA	Number of open-water patches in the entire river; see *IOAREA*.
NR	Number of reaches in branch while performing thermal computations.
QB(i)	Average flow rate of reach i ($m^3 s^{-1}$); $i = 1, 2, \ldots NR$.
QD(i)	Discharge at downstream end of reach i ($m^3 s^{-1}$); $i = 1, 2, \ldots NR$.
QLAT(i)	Lateral inflow discharge of reach i ($m^3 s^{-1}$); $i = 1, 2, \ldots NX$.
QLATI(i)	Lateral inflow discharge of reach i ($m^3 s^{-1}$); $i = 1, 2, \ldots NR$.
QU(i)	Discharge at upstream end of reach i ($m^3 s^{-1}$); $i = 1, 2, \ldots NR$.
RICE(i)	Ice roughness (Manning) of a reach i; $i = 1, 2, \ldots NR$.
RMUN(i)	Manning's roughness coefficient of a point i; $i = 1, 2, \ldots NX$.
RMUNI(i)	Fraction of an ice cover during the previous time step at reach i.
S(i)	Distance from node 1 to termination point of i^{th} Lagrangian moving point at the end of the time step (m); $i = 1, 2, \ldots NB$.
SF(i,1)	Frictional slope at net point i during the current time step; $i = 1, 2, \ldots NX$.
SF(i,2)	Frictional slope at net point i during the previous time step; $i = 1, 2, \ldots NX$.
T(i,1)	Channel top width at net point i during the current time step (ft); $i = 1, 2, \ldots NX$.
T(i,2)	Channel top width at net point i during the previous time step (ft); $i = 1, 2, \ldots NX$.
TB(i)	Average top width of river section i used in the ice computations (m); $i = 1, 2, \ldots NR$.
TD(i)	Downstream top width of river section i used in the ice computations (m); $i = 1, 2, \ldots NR$.
TFRA(i)	Thickness of frazil ice in reach i (m); $i = 1, 2, \ldots NR$.
THINI(i)	Thickness of initial ice cover in reach i (m); $i = 1, 2, \ldots NR$.

Table A2 (cont'd).

Variable	*Definition*
THPRO(i)	Thickness of initial ice cover of reach *i* computed using jam equations. This thickness is used to compute the length of progression for a given volume of ice (m); *i* = 1, 2,...*NR*.
TICE(i)	Sum of black and white ice thicknesses in reach *i* (m); *i* = 1, 2,...*NR*.
TLI(i)	Temperature of the lateral inflow *i* during the thermal computations.
TSUB(i)	Submerged thicknesses of the ice cover in reach *i* (m); *i* = 1, 2,...*NR*.
TU(i)	Upstream top width of river section *i* used in the ice computations (m); *i* = 1, 2,...*NR*.
TW(i)	Cross-sectional average water temperature at node *i* (°C). The same variable is used to express cross-sectional average frazil ice concentration at node *i* as a temperature. When *TW(I)* is negative, concentration is obtained by multiplying it by *FRCONV*.
TWXA(i)	Water temperature of node 1 at next time step (°C).
TWO(i,j)	Individual frazil concentration distributions of each of the open-water areas; *i* = node number; *j* = open-water patch counter; *i* = 1, 2,...*NB*; *j* = 1, 2,...*NOAREA*. This variable is used in subroutine *OPENLAGR*.
U(i,1)	Flow velocity at net point *i* during the current time step (ft^3s^{-1}); *i* = 1, 2,...*NX*.
U(i,2)	Flow velocity at net point *i* during the previous time step (ft^3s^{-1}); *i* = 1, 2,...*NX*.
UB(i)	Average river flow velocity in reach *i* ($m\ s^{-1}$); *i* = 1, 2,...*NR*.
WP(i)	Wetted perimeter of node *i* (ft); *i* = 1, 2,...*NX*.
WPI(i)	Wetted perimeter of node *i* during the previous time step (ft); *i* = 1, 2,...*NX*.
X(i)	Distance from node 1 to node *i* (m); *i* = 1 , 2,...*NR*.
ZD(i)	Height of the reference elevation at the downstream end of the reach *i* (m); *i* = 1, 2,...*NR*.
ZU(i)	Height of the reference elevation at the upstream end of the reach *i* (m); *i* = 1, 2,...*NR*.

REPORT DOCUMENTATION PAGE

Form Approved
OMB No. 0704-0188

1. AGENCY USE ONLY (Leave blank)	2. REPORT DATE	3. REPORT TYPE AND DATES COVERED
	September 1991	

4. TITLE AND SUBTITLE

Numerical Model for Forecasting Ice Conditions on the Ohio River

5. FUNDING NUMBERS

River Ice Management Program
Work Unit CW32227

6. AUTHORS

Hung Tao Shen, Goranka Bjedov, Steven F. Daly and A. M. Wasantha Lal

7. PERFORMING ORGANIZATION NAME(S) AND ADDRESS(ES)

Clarkson University
Potsdam, New York

8. PERFORMING ORGANIZATION REPORT NUMBER

9. SPONSORING/MONITORING AGENCY NAME(S) AND ADDRESS(ES)

Sponsoring Agency:
Office of the Chief of Engineers
Washington, D.C. 20314-1000

Monitoring Agency:
U.S. Army Cold Regions Research and Engineering Laboratory
72 Lyme Road
Hanover, New Hampshire 03755-1290

10. SPONSORING/MONITORING AGENCY REPORT NUMBER

CRREL Report 91-16

11. SUPPLEMENTARY NOTES

12a. DISTRIBUTION/AVAILABILITY STATEMENT

Approved for public release; distribution is unlimited.

Available from NTIS, Springfield, Virginia 22161

12b. DISTRIBUTION CODE

13. ABSTRACT (*Maximum 200 words*)

A numerical model, RICEOH, for simulating flow and ice conditions in a dendritic river system is developed. The flow computations use a double-sweep algorithm for unsteady shallow-water wave equations. The distributions of water temperatures and ice concentration are determined using a Lagrangian–Eulerian scheme. The formation of an ice cover is modeled using existing equilibrium ice jam theories. Frazil ice deposition and erosion are modeled by a simple critical-velocity criterion. The thermal growth and decay of an ice cover is calculated by a quasi-steady finite-difference method. The model is applied to the Ohio River system between Pittsburgh, Pennsylvania, and Meldahl, Ohio. Comparisons with field observations show that the model can provide good simulation for ice conditions.

14. SUBJECT TERMS

Computer models | Ohio River | River ice models | Winter navigation

15. NUMBER OF PAGES

61

16. PRICE CODE

17. SECURITY CLASSIFICATION OF REPORT	18. SECURITY CLASSIFICATION OF THIS PAGE	19. SECURITY CLASSIFICATION OF ABSTRACT	20. LIMITATION OF ABSTRACT
UNCLASSIFIED	UNCLASSIFIED	UNCLASSIFIED	UL

NSN 7540-01-280-5500

☆ U. S. GOVERNMENT PRINTING OFFICE: 1991--600-063--42030

Standard Form 298 (Rev. 2-89)
Prescribed by ANSI Std. Z39-18
298-102